The University of Jordan

School of Engineering

Chemical Engineering Department

Chemical Engineering Laboratory (2) (0915461)

Experiment Number (1)

Vapor-Liquid Equilibrium

Type of the report: short report

Done by:

Instructor:

Eng. Rula Mohammad & Eng. Arwa Sandoqa

Performing Date: 18 / 04 / 2023

Submitting Date: 2/ 05 / 2023

Abstract

In this experiment, the binary system equilibrium data for n-hexane and toluene were collected to construct a T-XY diagram and calculate the activity coefficient. The activity coefficient was calculated using the Van Laar model. If the activity coefficient deviates significantly from unity, the mixture is not ideal and will not obey Raoult's law.

Table Of Contents

Table of Figures

Table of Tables

Results

Table 1:Properties of toluene and hexane

Runs	temp °C	P sat T	Psat H	density Tv	density Hv	density T_L	density H_L
1	105.4	653.7		2.73	2.546	786.1	575.56
2	95	477.02	1613.5	2.815	2.624	796.8	587.088
3	86.3	360.47	1272.64	2.88	2.693	805.5	596.45
4	81.5	306.708	1110.07	2.93	2.733	810.3	601.56
5	78.5	276.527	1016.9	2.959	2.759	813.3	604.7
1	70.5	207.56	798.15	3.036	2.83	821.1	612.88
2	67.5	185.66	726.36	3.066	2.858	824.1	615.9
3	64.6	166.29	661.88	3.095	2.89	826.9	618.9
4	60.5	141.755	578.51	3.138	2.92	830.8	623
5	55.5		448.32	3.192	2.97	835.6	627.9

Table 2:Liquid phase properties of hexane and toluene

Runs	temp	RI for liq	vol-H%	ύ H liq(m^3/mol)	ύ T liq(m^3/mol)	Xh	Xt
1	105.4			0.1497	0.1172	0.0000	1.0000
2	95	1.481	0.1300	0.1468	0.1156	0.1053	0.8947
3	86.3	1.4804	0.1350	0.1445	0.1144	0.1100	0.8900
4	81.5	1.4774	0.1600	0.1433	0.1137	0.1313	0.8687
5	78.5	1.4636	0.2750	0.1425	0.1133	0.2317	0.7683
1	70.5	1.433	0.5300	0.1406	0.1122	0.4737	0.5263
2	67.5	1.4212	0.6283	0.1399	0.1118	0.5746	0.4254
3	64.6	1.4051	0.7625	0.1392	0.1114	0.7198	0.2802
4	60.5	1.3942	0.8533	0.1383	0.1109	0.8235	0.1765
5	55.5			0.1373	0.1103	1.0000	0.0000

Table 3:Vapor phase properties of hexane and toluene

Runs	temp	RI forvap	vol-H%	ύ H vap(m^3/mol)	ύ T vap(m^3/mol)	Yh	Yt
1	105.4			33.8492	33.7509	0.0000	1.0000
2	95	1.4401	0.4708	32.8430	32.7318	0.4700	0.5300
3	86.3	1.4365	0.5008	32.0015	31.9931	0.5008	0.4992
4	81.5	1.4474	0.4100	31.5331	31.4471	0.4093	0.5907
5	78.5	1.435	0.5133	31.2360	31.1389	0.5126	0.4874
1	70.5	1.4801	0.1375	30.4523	30.3491	0.1371	0.8629
2	67.5	1.4832	0.1117	30.1540	30.0522	0.1113	0.8887
3	64.6	1.4538	0.3567	29.8201	29.7706	0.3563	0.6437
4	60.5	1.386	0.9217	29.5137	29.3627	0.9213	0.0787
5	55.5			29.0168	28.8659	1.0000	0.0000

Table 4:Activity coefficient using modified Raoul's law.

Runs	γ1	γ2
1		1.037173
2	1.875245	0.841993
3	2.425982	1.055015
4	1.903678	1.503103
5	1.475095	1.5555
1	0.245873	5.355259
2	0.180848	7.62916
3	0.50702	9.367389
4	1.311208	2.132385
5	1.512313	

Table 5:Activity coefficients using van laar modeling.

Runs	ln γ1	ln γ2	ln(γ1/γ2)	γ1	γ2
1	0.8080			2.2434	
2	0.7424	0.0038	0.7386	2.1010	1.0038
3	0.7394	0.0041	0.7352	2.0946	1.0042
4	0.7252	0.0061	0.7191	2.0651	1.0061
5	0.6549	0.0219	0.6330	1.9249	1.0221
1	0.4563	0.1358	0.3205	1.5783	1.1454
2	0.3609	0.2420	0.1189	1.4346	1.2737
3	0.2138	0.5185	-0.3047	1.2384	1.6796
4	0.1097	0.8771	-0.7674	1.1159	2.4038
5		2.1991			9.0164

Using thermosolver software: van laar coefficient: A12=0.808007, A21=2.19905

Table 6:Activity coefficients using Two-suffix Margules Equation

Runs	ln γ1	ln γ2	γ1	γ2
1	1.0765	0.0000	2.934479	1
2	0.8617	0.0119	2.367231	1.012012
3	0.8528	0.0130	2.346155	1.013104
4	0.8123	0.0186	2.253158	1.018741
5	0.6355	0.0578	1.887978	1.059481
1	0.2982	0.2415	1.34748	1.273187
2	0.1948	0.3555	1.21506	1.426838
3	0.0845	0.5578	1.088183	1.746813
4	0.0335	0.7300	1.034118	2.075066
5	0.0000	1.0765	1	2.934479

Using thermosolver software: Two-suffix Margules coefficient: A12=1.07653

Figures

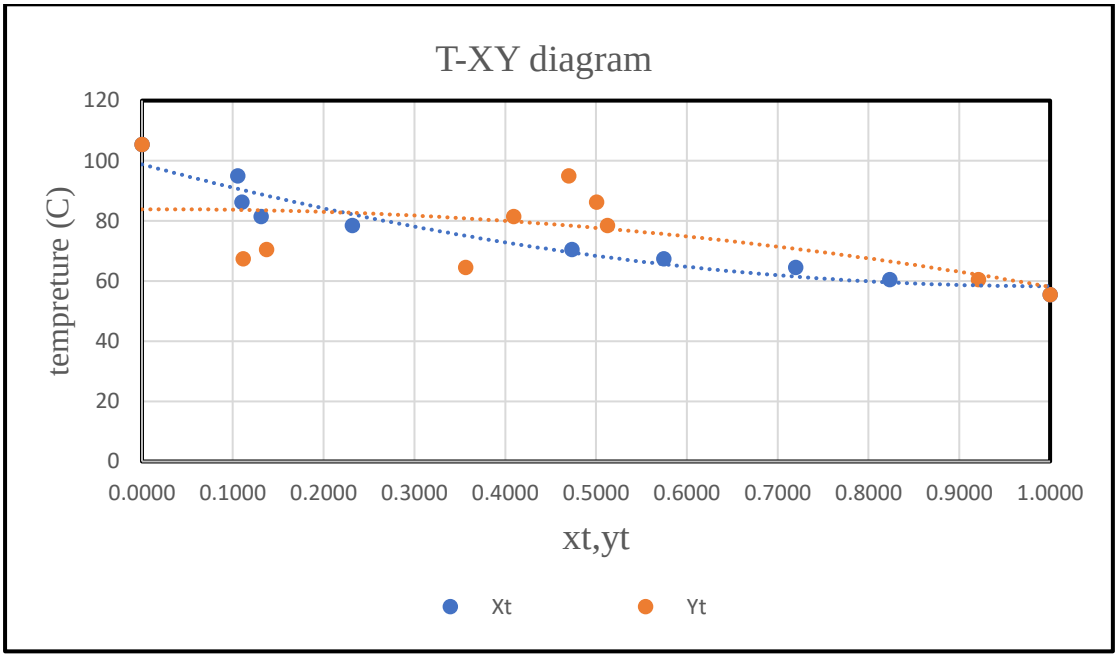

Figure 1: T-XY diagram

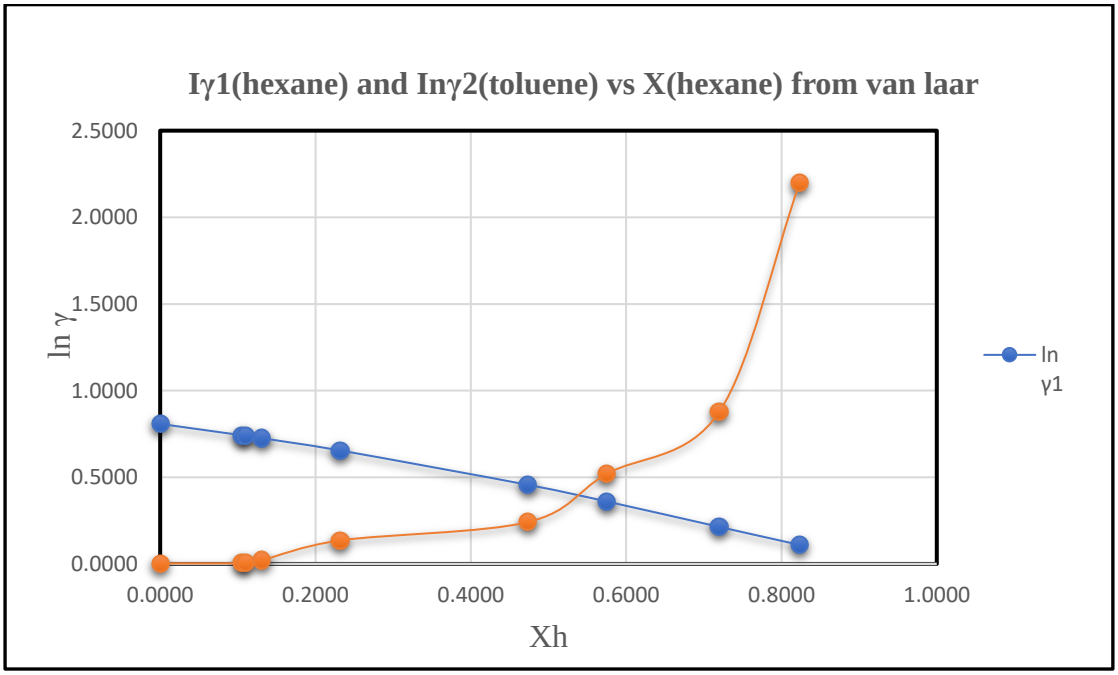

Figure 2:Iy1(hexane) and Iny2(toluene) vs X(hexane) from van laar

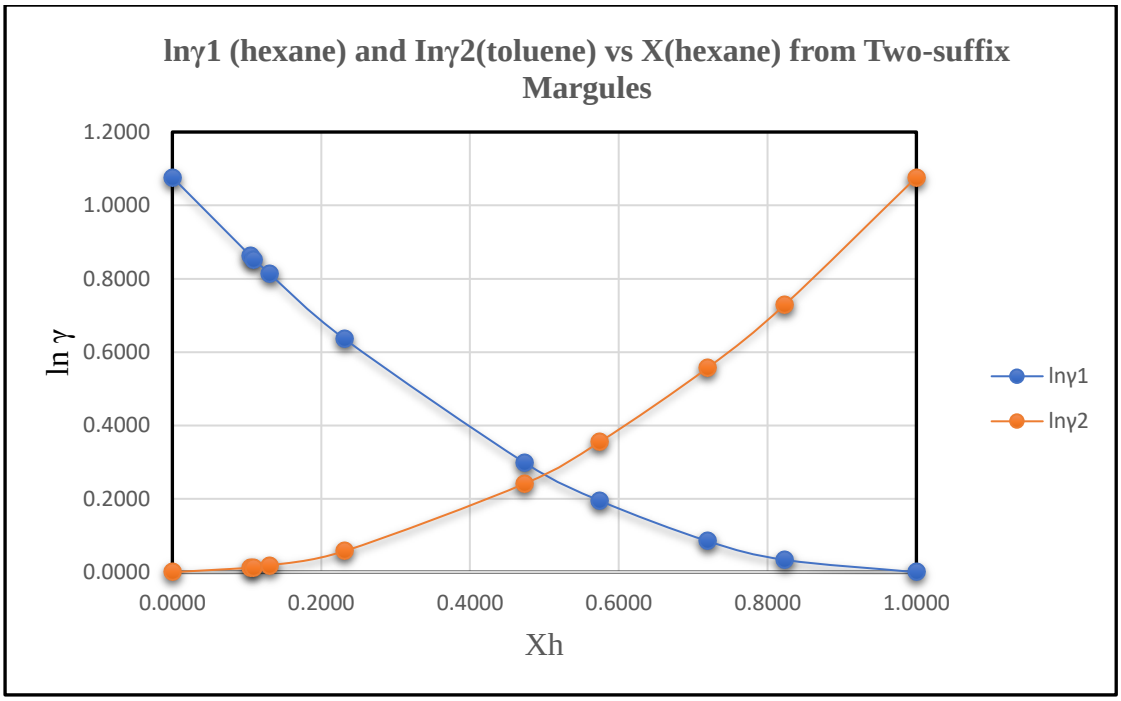

Figure 3:lnγ1 (hexane) and Inγ2(toluene) vs X(hexane) from Two-suffix Margules

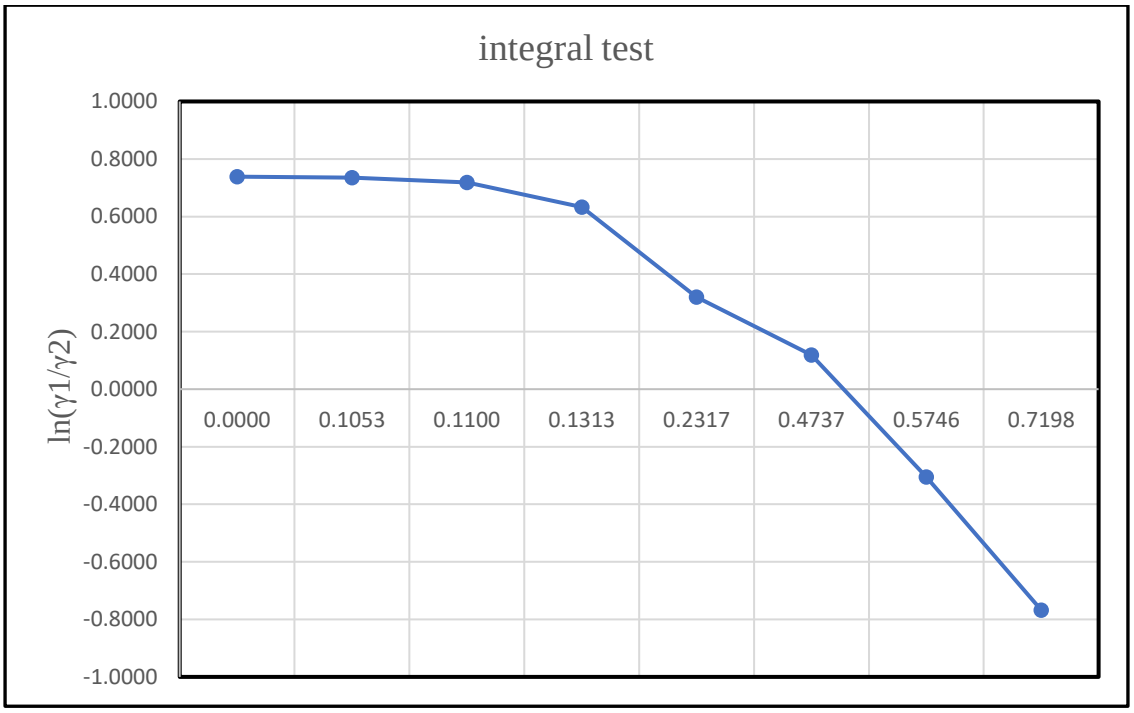

Figure 4:The consistency of data using integral test.

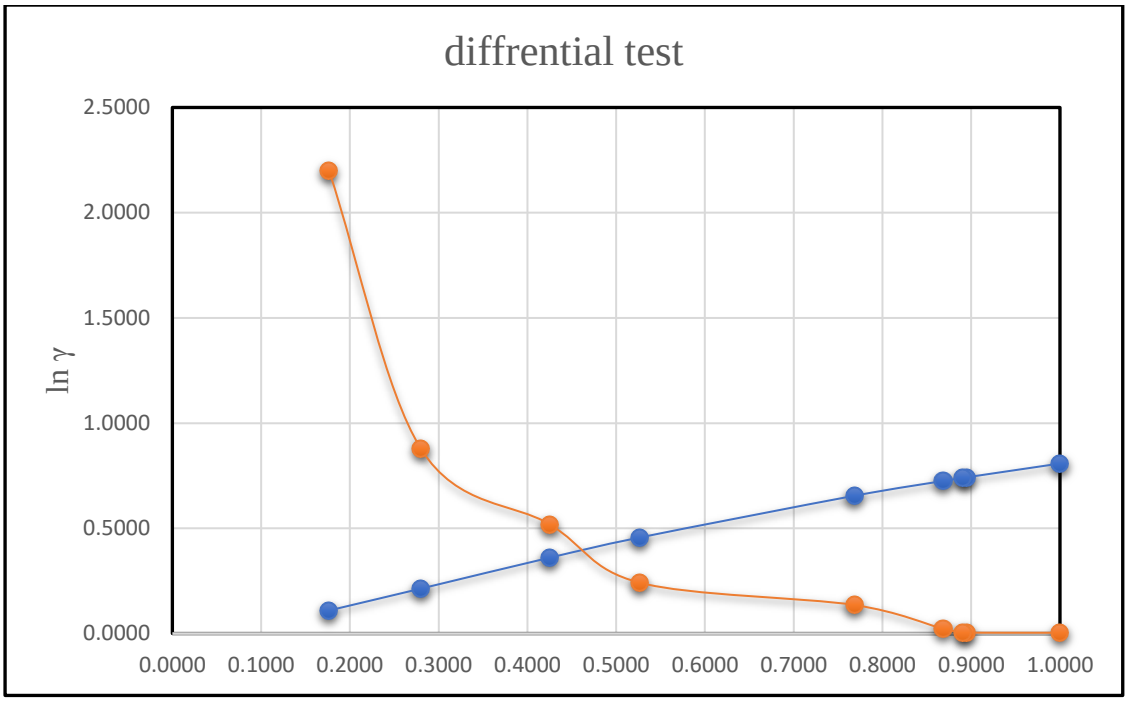

Figure 5:The consistency of data using differential test.

Results from thermosolver software:

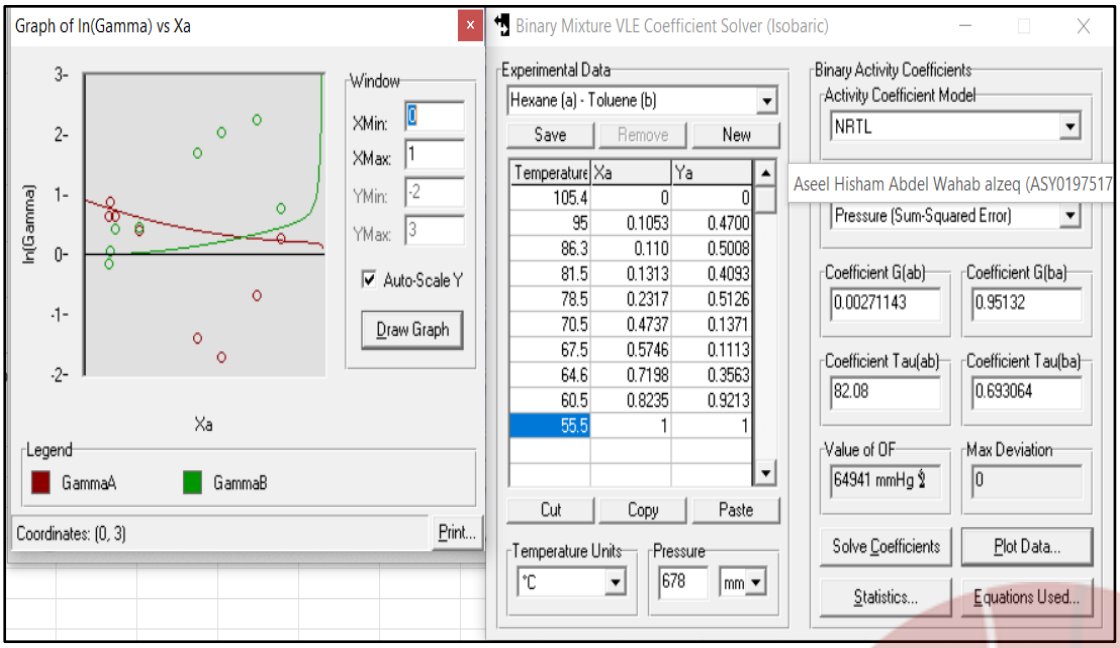

Figure 6: NRTL

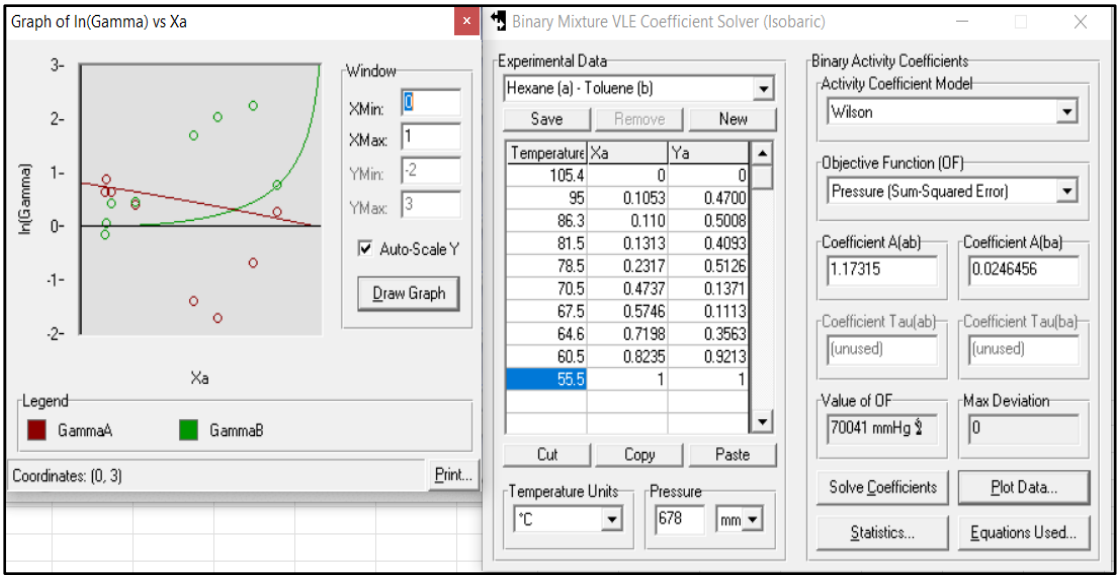

Figure 7:Wilson

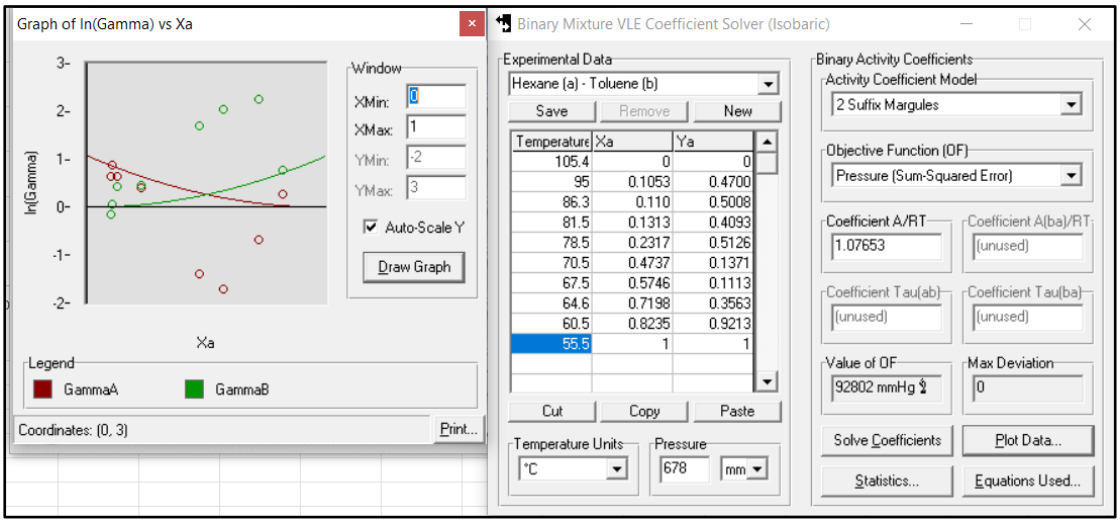

Figure 8:Two-suffix Margules

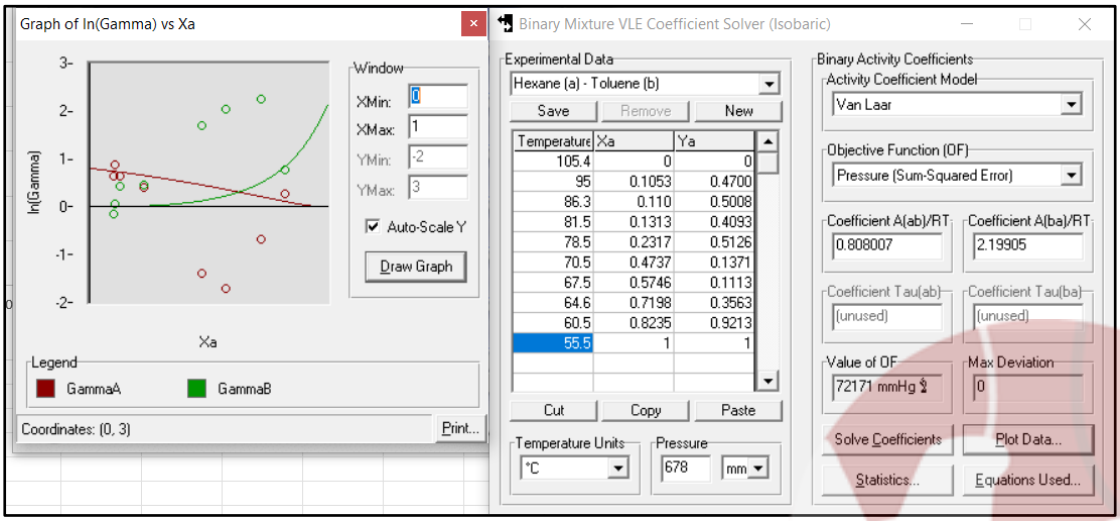

Figure 9:Van laar

Discussion

This experiment is carried out to investigate the relationship between vapor and liquid of binary mixture (n-hexane -toluene) at equilibrium at 1 atm . The composition of the liquid phase will be designated by the mole fraction of the more volatile component (n-hexane), which has lower boiling point, represented by x. The mole fraction of the other component (Toluene) is of course 1- x. and this solution is a non-ideal solution because of the difference of hexane and toluene structural interaction .

mixture of n-hexane-water with known composition is initially fed into the evaporator. When the heater is switched on, the mixture will start to boil. The mixture vapour will rise and will be cooled down by the condenser at the top of the evaporator. As the vapour starts to condense, the liquid falls back into the evaporator. The system will stabilize and finally reach an equilibrium state when temperature remains constant. Samples of vapour and liquid are taken to determine their compositions.

Based on the data recorded the graph of T-xy can be plotted. This graph represents data for 2 component (Binary) system. The system is Temperature against Mole fraction of vapour and Temperature against Mole fraction of liquid . X-axis is the composition of component 1 mvc (hexane here), Y-axis is the temperature of the system. Hence, we can also notice at x = 1 (pure n-hexane) the Temperature of the system is approximately 58 C and at x =0 (pure toluene), the temperature is approximately 105 C

the activity coefficient is a measure of how much a solution differs from an ideal solution, The activity coefficient can be calculated from different methods, some of which are: The Modified Raoult's Law, Van Laar, and Two Suffix Margules, NRTL, Wilson, and UNIFAC)

Then the graph of activity coefficient based on table 5 The figure (3) was plotted, we can see, it gives a good approximation of gamma1 and gamma2, the increasing curve is the curve that represents the activity coefficient for Hexane and will decreasing for toluene because the effectiveness of the component in the mixture. The figure shows when we have a pure toluene (x = 0), the activity coefficient of toluene had the highest value while the activity coefficient of hexane equal zero

At (x=1)pure n-hexane the activity coefficient had the lowest value while the activity coefficient of toluene equal 1

Consistency of data (The thermodynamic consistency test) It is a way to check whether a given set of experimental VLE data satisfies the fundamental Gibbs–Duhem equation such as integral test and differential test. According to the experimental (graphical & tabular) results; there are some errors obtained in experimental data if we compare it with experiments that have been done in literature, here are some reasons for that:

• The Equilibrium still and refractometer, which have been used in this experiment, have systematic errors.

• There are some impurities in the system which are affecting the boiling temperature.

• There were some losses in the vapor & liquid when the refractive index was measured.

• Heat losses to the ambient and the measuring devices have less accuracy (calibration of thermocouple).

• Personal errors, not accurate reading from the refractometer and the calibration curve.

Conclusion

By conducting the experiments on different composition of mixture, we can conclude that:

The experiment was carried out to determine the vapor liquid equilibrium conditions for the binary Toluene - Hexane system and correlate the results for use in the analysis of the distillation column.

- T-x-y diagram shows the composition of phase in binary mixture depending on the temperature of the system at constant pressure. And the tie line indicates the equilibrium of liquid and vapor mixture at the same temperature and pressure.
- Since the binary (n-hexane -toluene) system is not ideal due to difference in shape size and molecular interaction, the mixture does not obey Raoult's law, and the activity coefficient is far from unity.
- The activity coefficient is a function of temperature, pressure, and composition, which is used to account for the deviation from ideality, ideal mixture has been calculated using different methods (modified Raoul's law, van Laar modeling, and Two-suffix Margules Equation).
- If the activity coefficient equal 1 the mixture obeys Raoult's law, and if it's greater than 1 there are a positive deviation from Raoult's law due to that vapor pressure of the mixture is higher than the vapor pressure for each component in pure form, which means that the mixture is more volatile that both components in pure form.
- The integral test is used to check the consistency of data, when plotting $\ln(\gamma 1/\gamma 2)$ versus x1. the area under the curve should be equal zero. From figure (4), the area under the curve cannot be determined, the test is passed.

Recommendations

- Gloves should exist to prevent chemicals from touching the hands.
- It is recommended to take a reading of the boiling temperature directly from a thermocouple when it remains constant, because it is affected by room temperature.
- The measuring devices must be cleaned using acetone to get perfect reading.
- To guarantee better readings, the refractometer's light source needs to be stronger.
- Personal errors arise in reading the refract meter because the fourth last digit is read by person, so be careful.

References

1) Chemical engineering laboratory “2” (0915461); University of Jordan; faculty of engineering and Technology; Department of Chemical engineering.

Appendix

- Sample of calculations:

  - **liquid phase properties :**

    AT, T = 95 C
    -RI = 1.481
    -Density of H = 587.088
    -Density of T =796.8
    -MW H =0.08618
    -MW T = 0.09214

    1) **Vol-H%** = $(\frac{RI-1.4966}{-0.0021})/100 = (\frac{1.481-1.496}{-.0.0021})/100 = 0.1300$

    2) **ύ H liq(m^3/mol)** = $\frac{\text{MW H}}{\text{Density of H}*1000} = \frac{0.08718}{587.088*1000} = 0.1468$

    3) **ύ T liq(m^3/mol)** = $\frac{\text{MW T}}{\text{Density of T}*1000} = \frac{0.09214}{796.8*1000} = 0.1156$

    4) **Xh**= $\frac{(\text{Vol}-\text{H\%}/\text{ύ H liq})}{(\text{Vol}-\text{H\%}/\text{ύ H liq})+((1-\text{Vol}-\text{H\%})/\text{ύ T liq})} = \frac{(0.1300/0.1468)}{(0.1300/1.468)+((1-0.1300)/0.1156)} = 0.1053$

    5) **Xt** = 1-Xh = 1-0.1053 = 0.8947

  - **Vapor phase properties :**

    AT, T = 95 C
    -RI = 1.4401
    -Density of H = 2.624
    -Density of T = 2.815
    -MW H =0.08618
    -MW T = 0.09214

    1) **Vol-H%** = $(\frac{RI-1.4966}{-0.0021})/100 = \frac{1.4401-1.496)}{-0.0021}/100 = 0.4708$

    2) **ύ H vap (m^3/mol)** = $\frac{\text{MW H}}{\text{Density of H}*1000} = \frac{0.08718}{2.624*1000} = 32.8430$

    3) **ύ T vap (m^3/mol)** = $\frac{\text{MW T}}{\text{Density of T}*1000} = \frac{0.09214}{2.815*1000} = 32.7318$

    4) **Yh**= $\frac{(\text{Vol}-\text{H\%}/\text{ύ H vap})}{(\text{Vol}-\text{H\%}/\text{ύ H vap})+((1-\text{Vol}-\text{H\%})/\text{ύ T vap})} = \frac{(0.4708/32.8430)}{(0.4708/32.8430)+((1-0.4708)/32.7)} = 0.4700$

    5) **Yt** = 1-Yh = 1-0.4700 = 0.5300

From Raoult law:

1) **γ1**= $\frac{Yh*678}{Xh*1613.5} = 1.875$
2) **γ2**= $\frac{Yt*678}{Xt*477.02} = 0.842$

From van lar :

1) **lnγ1**= $\frac{A12}{((1+(A12/A21))*(Xh/Xt))^2} = \frac{0.80801}{((1+(0.80801/2.19905))*(0.1053/0.8947))^2} = 0.7424$

2) **lnγ2**= $\frac{A21}{((1+(A21/A12))*(Xt/Xh))^2} = \frac{2.19905}{((1+(2.19905/0.80801))*(0.8947/0.1053))^2} = 0.0041$

3) **γ1**=$e^{\ln\gamma 1} = 2.1010$

4) **γ2**=$e^{\ln\gamma 2} = 1.0038$

5) **ln** $\frac{\gamma 1}{\gamma 2} = 0.7386$

From 2 suffix margulase :

1) **ln γ1**=A12 *Xt^2 = 1.07653 * $0.8947^2 = 0.8617$

2) **ln γ2**=A12 *Xh^2 = 1.07653 * $0.1053^2 = 0.0119$

3) **γ1**=$e^{\ln\gamma 1} = 2.367$

4) **γ2**=$e^{\ln\gamma 2} = 1.012$

- Data sheet:

Version no. 7 September, 2020

Vapor-Liquid Equilibrium Data Sheet

Atmospheric pressure: 678 mmHg.

Mixture used	Equilibrium Temperature	RI of vapor	RI for liquid
120 ml T	105.4	—	—
120 mL T + 20 mL h	95	1.44	1.497
120 mL T + 40 mL h	86.3	1.4365	1.4804
120 mL T + 60 mL h	81.5	1.4474	1.4774
120 mL T + 80 mL h	78.5	1.4350	1.4636
120 mL H	55.5	—	—
120 mL H + 20 mL T	60.5	1.3860	1.3942
120 mL H + 40 mL T	64.6	1.4538	1.4051
120 mL H + 60 mL T	67.5	1.4832	1.4212
120 mL H + 80 mL T	70.5	1.4801	1.4330

Instructor signature:	
Date: 11/4/2023	

Page 8 of 48

The University of Jordan

School of Engineering

Chemical Engineering Department

Chemical Engineering Laboratory (2) (0915461)

Experiment Number (2)

Liquid-Liquid Equilibrium

Type of the report: short report

Done by:

Instructor:

Eng. Rula Mohammad & Eng. Arwa Sandouqa

Performing Date: 21 / 03 / 2023

Submitting Date: 28 / 03 / 2023

Abstract

The objective of this experiment is to study mass transfer process by means of liquid-liquid equilibrium data for ternary system involve "Water (solvent I), Acetone (solute), Toluene (solvent II)" in the range of different volumes / mass fractions. Results showed the mutual solubility curve for the ternary system on an equilibrium triangle and constructed the tie line corresponding to each mixture and when it compared with published values unfortunately there are some of error. Liquid - Liquid extraction process needs for Liquid - Liquid equilibrium data so it was concluded that the solvent must be insoluble or soluble to a limited extent only, in the solution to be extracted and the experiment shows that acetone is more soluble in water.

Table Of Contents

Table Of Figures

Table Of Tables

Results

Table 1 : Densities of each compound at 20°C in g/ml

Water	Toluene	Acetone
0.9982	0.8669	0.7900

❖ **Ternary mutual solubility curve formation**

1- Water rich phase

Table 2 : Water-Rich Phase calculated parameters

Volume of A (ml)	Volume of W (ml)	Volume of T (ml)	mass of A (g)	mass of W (g)	mass of T (g)	Total mass (g)	X_A	X_W	X_T
5	20	0.1	3.95	19.964	0.0867	24.0007	0.1646	0.8318	0.0036
10	20	3.3	7.9	19.964	2.8608	30.7248	0.2571	0.6498	0.0931
15	20	1.5	11.85	19.964	1.3004	33.1144	0.3579	0.6029	0.0393
10	10	0.9	7.9	9.982	0.7802	18.6622	0.4233	0.5349	0.0418
20	10	1.9	15.8	9.982	1.6471	27.4291	0.5760	0.3639	0.0600
30	10	3.5	23.7	9.982	3.0342	36.7162	0.6455	0.2719	0.0826

2- Toluene rich phase

Table 3 : Toluene-Rich Phase calculated parameters

Volume of A (ml)	Volume of T (ml)	Volume of W (ml)	mass of A (g)	mass of W (g)	mass of T (g)	Total mass (g)	X_A	X_W	X_T
5	20	0.3	3.95	0.29946	17.3380	21.5875	0.1830	0.0139	0.8032
10	20	0.4	7.9	0.39928	17.3380	25.6373	0.3081	0.0156	0.6763
15	20	0.4	11.85	0.39928	17.3380	29.5873	0.4005	0.0135	0.5860
10	10	0.6	7.9	0.59892	8.6690	17.1679	0.4602	0.0349	0.5050
20	10	0.4	15.8	0.39928	8.6690	24.8683	0.6353	0.0161	0.3486
30	10	2.8	23.7	2.79496	8.6690	35.1640	0.6740	0.0795	0.2465

Figures (1)

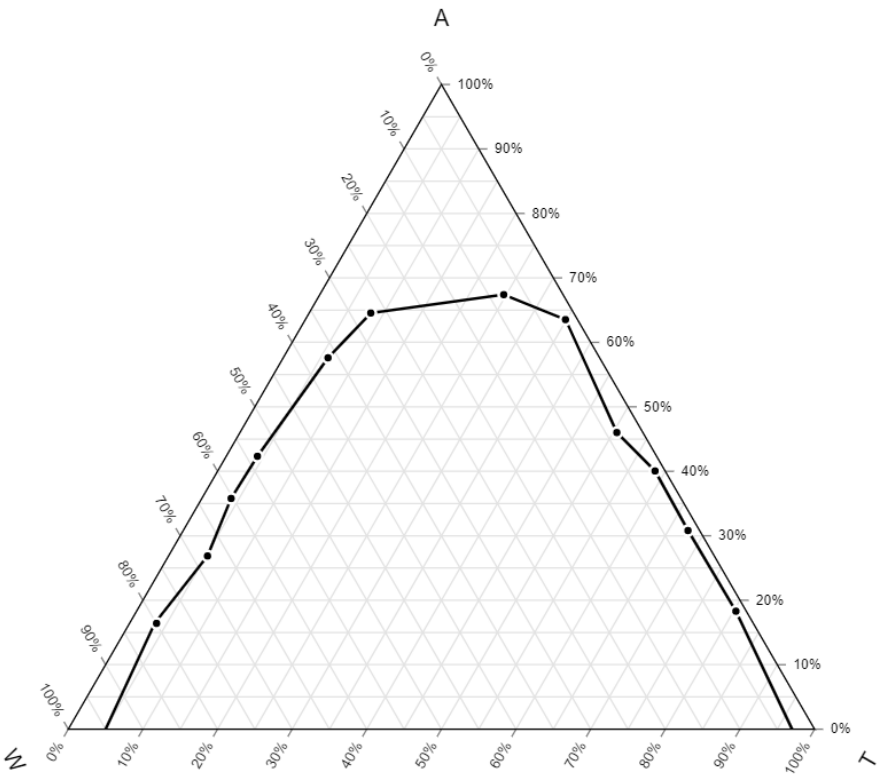

Figure 1 : Mutual Solubility Curve for Ternary System.

❖ **Tie Line determination:**

Table 4 : Tie-Line determination data

Sample No.	Volume of W (ml)	Volume of T (ml)	Volume of A (ml)	mass of A (g)	mass of W (g)	mass of T (g)	Total mass (g)	X_A	X_W	X_T
1	20	15	15	11.85	19.964	13.0035	44.8175	0.2644	0.4455	0.2901
2	26	17	8	6.32	25.9532	14.7373	47.0105	0.1344	0.5521	0.3135
3	19	29	3	2.37	18.9658	25.1401	46.4759	0.0510	0.4081	0.5409

Table 5: Tie-line composition and othmer-Tobias Correlation

Sample No.	RI		Raffinate		Extract		Othmer -Tobias correlation	
	Water layer	Toluene layer	X_A	X_W	X_A	X_T	log((1-b)/b)	log((1-a)/a)
1	1.3540	1.4620	0.2892	0.7108	0.2778	0.7222	-0.3905	-0.4150
2	1.3365	1.4999	0.0200	0.9800	0.0030	0.9970	-1.6902	-2.5270
3	1.3416	1.4942	0.0985	0.9015	0.0393	0.9607	-0.9617	-1.3887

Figures (2)

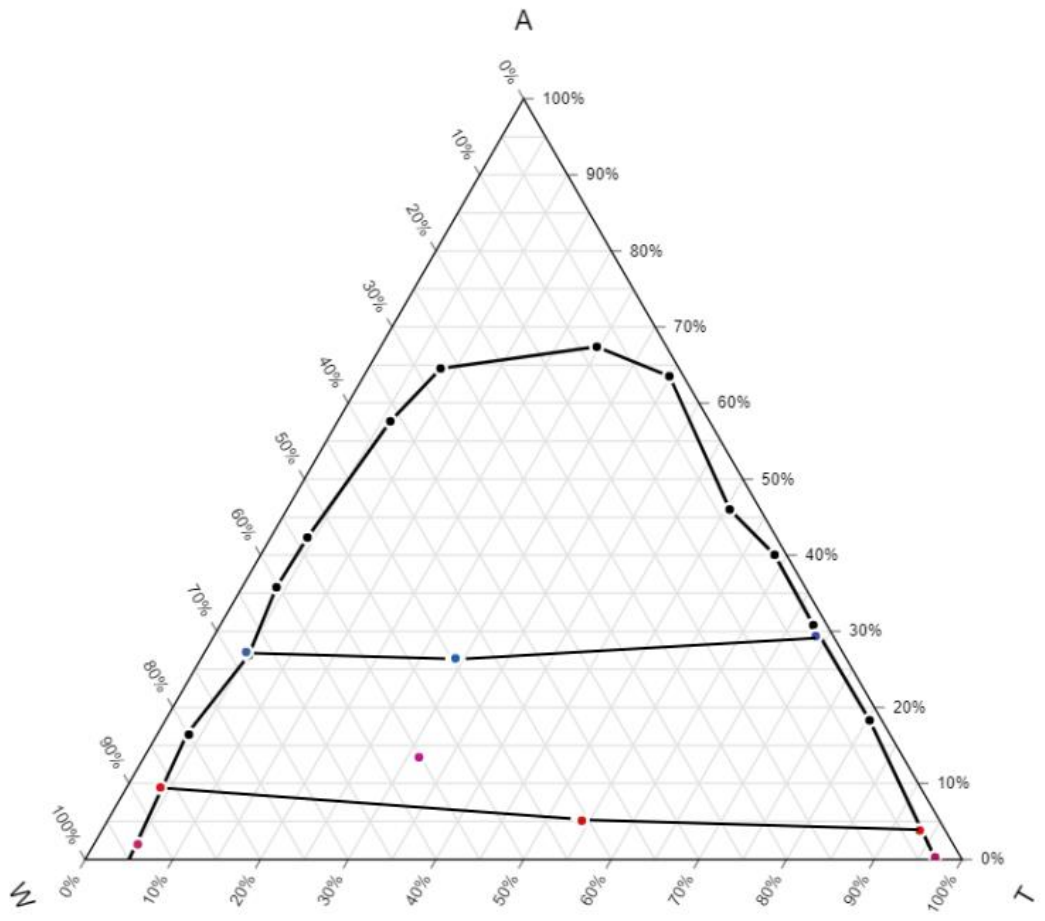

Figure 2 : Ternary phase diagram with tie-lines

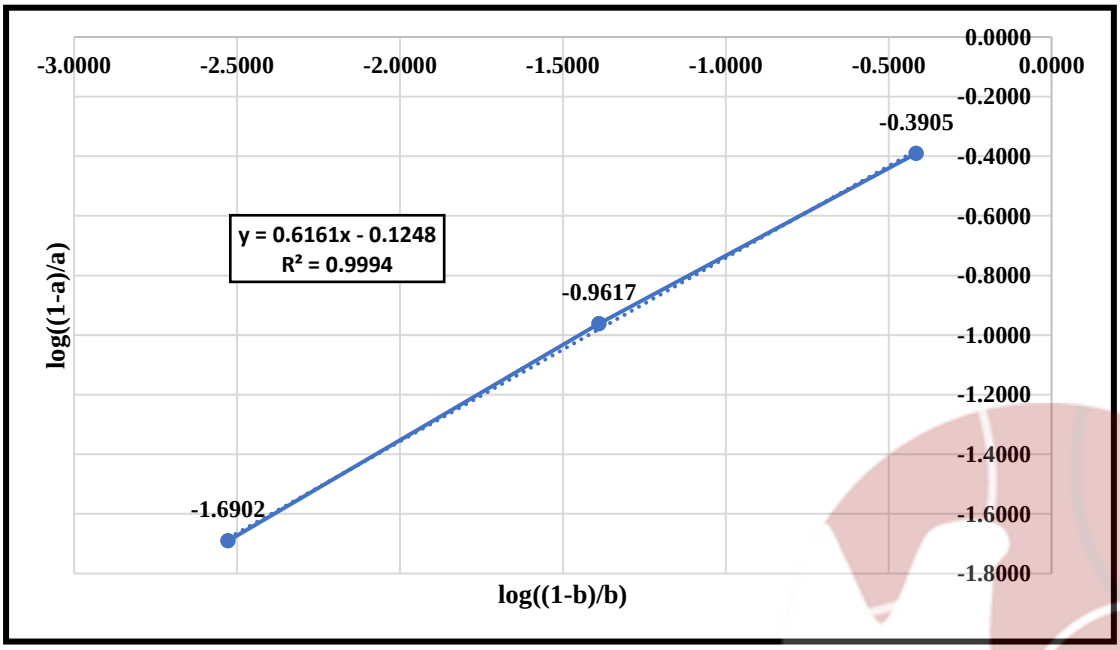

Figure 3 : Linearity Check (Othmer-Tobias Correlation)

Discussion

A phase diagram is a type of chart used to show conditions (pressure, temperature, volume, etc.) at which thermodynamically distinct phases (such as solid, liquid, or gaseous states) occur and coexist at equilibrium.

A ternary phase diagram is a type of phase diagram which represents a three-component system conveniently presented in an equilateral triangle, where each side corresponds to an individual binary system. It also shows the equilibrium states between the raffinate and extract layers after the extraction process. There is also a mutual solubility curve, which separates the one-phase mixture (homogenous) from the two-phase mixture. Inside this curve can be seen isotherms that represent the equilibrium tie-lines.

In this experiment, the analyzed system made up of acetone, toluene and water all in the liquid phase. After gathering experimental data, a ternary phase diagram is plotted, and an individual precise tie line is used to represent each state of equilibrium.

As seen in table (2), results for water-rich phase are obtained after six samples of titrating acetone and water mixtures against toluene, the end point of titration is when cloudiness appeared, which indicates that the solution has changed from a one-phase to a two-phase region. The data is then plotted on a ternary diagram to create the water rich side of the solubility equilibrium curve. The same procedure is carried out in table (3), where results for toluene-rich phase are obtained by titrating acetone and toluene mixtures against water, where turbidity is considered as titration end-point.

Consequently, a ternary phase diagram is plotted. As seen in figure (1); the six samples' results were used as points in order to plot the solubility curve. The best fitted line is drawn to indicate the equilibrium solubility curve, some points were scattered which is most probably a result of personal error from inaccurate reading of the burette.

The plait point, which is a point where the composition of the toluene- rich phase and the water-rich phase are equal, should be determined but it is difficult to identify due to sample composition range.

Three samples are mixed, settled, and then analyzed under a refractometer in order to read the refractive index (RI) to determine the composition and generate the tie-lines.

As seen in figure (2), the 1st and 3rd compositions of sample are plotted as two equilibrium isotherms (tie-lines). It leans slightly into the water-rich phase, which indicates that acetone is more soluble or more miscible in the water-rich phase rather than the toluene-rich phase. There was an error in the 2nd composition and the tie line can't be determined.

As seen in figure (3), The Othmer-Tobias correlation is used to check the linearity of these experimental data with a slope of 0.6161 and an intercept of -0.1248 and R^2 = 0.9994.

Conclusion

We got ternary diagram for "Water (solvent I), Acetone (solute), Toluene (solvent II)" system and test a result by Linearity Check (Othmer-Tobias Correlation) and got a linear curve that mean the tie line real and true. The charting of the ternary phase diagram and the scattered points for the mutual solubility curve have obviously been impacted by some errors. A higher number of samples must have been taken in order to identify the plait point, which is a point signifying equality of the water-rich phase and the toluene-rich phase but is not identified in this experiment. To sum up, the key tool used in this experiment to detect the boundary between the one-phase and two-phase regions was cloudiness and turbidity.

References

1) Chemical engineering laboratory "2" (0915461); University of Jordan; faculty of engineering and Technology; Department of Chemical engineering.
2) Toluene Solvent Properties, Acetone Solvent Properties, Water Solvent Properties
   https://macro.lsu.edu/HowTo/solvents/acetone.htm

   https://macro.lsu.edu/howto/solvents/toluene.htm

   https://macro.lsu.edu/howto/solvents/water.htm

Appendix

❖ Sample of calculation:

➔ **For table (1):**

- Density for water @ 20℃ = 0.9982
- Density for toluene@ 20℃ = 0.8669
- Density for Acetone @ 20℃ = 0.7900

❖ **(The calculations for the first row of each table will be shown)**

- Mass Density * Volume
- mass of component Mass fraction = - total mass
- Total mass = Mass of water + Mass of Toluene + Mass of Acetone

➔ **Ternary mutual solubility curve formation**

1- For water rich phase (from table 2):

- Volume of **Water** = 20.00 ml.
- Density of Water at 20 °C = 0.9982 g/ml.
- Mass of Water = 20.00 ml * 0.9982 g/ml = 19.964 g
- Volume of **Acetone** = 5.00 ml.
- Density of Acetone at 20 °C = 0.7900 g/ml.
- Mass of Acetone 5.00 ml *0.7900g/ml = 3.95g
- Volume of **Toluene** = 0.1 ml.
- Density of Toluene at 20 °C = 0.8669 g/ml.
- Mass of Toluene = 0.1 ml * 0.8669 g/ml = 0.08669 g
- **Total mass** =19.964 + 3.95 + 0.08669 = 24.0007 g
- **Water** mass fraction = $\frac{19.964\ g}{24.0007g}$ = 0.8318 g
- **Acetone** mass fraction = $\frac{3.95\ g}{24.0007\ g}$ = 0.1646 g
- **Toluene** mass fraction = $\frac{.08669\ g}{24.0007g}$ = 0.0036 g

2- For Toluene rich phase (from table 3):

- Volume of **water** = 0.30 ml
- Density of water @20 ℃ = 0.9982 g /ml
- Mass of water = 0.30*0.9982 = 0.29946 g
- Volume of **Acetone** = 5.00 ml.
- Density of Acetone at 20 °C = 0.7900 g/ml.
- Mass of Acetone = 5.00 ml *0.7900g/ml = 3.95g

- Volume of **Toluene** = 20 ml.
- Density of Toluene at 20 °C = 0.8669 g/ml.
- Mass of Toluene = 20 ml * 0.8669 g/ml =17.338g
- **Total mass** = 0.29946 + 3.95 + 17.338 = 21.5875 g
- **Water** mass fraction = $\frac{.29946\ g}{21.5875g}$ = 0.0139g
- **Acetone** mass fraction= $\frac{3.95\ g}{21.5875\ g}$ =.1830 g
- **Toluene** mass fraction= $\frac{17.338\ g}{21.5875g}$ =.8032 g

➔ **Tie-line determination:**

❖ **Tie-line determination (from table 4):**

- Volume of **water** =15 ml
- Density of water @ 20 ℃ = 0.9982 g /ml
- Mass of water = 15*0.9982 = 19.964 g
- Volume of **Acetone** = 15 ml.
- Density of Acetone at 20 °C = 0.7900 g/ml.
- Mass of Acetone =15 ml *0.7900g/ml =11.85g
- Volume of **Toluene** = 15ml.
- Density of Toluene at 20 °C: 0.8669 g/ml.
- Mass of Toluene = 15 ml * 0.8669 g/ml =13.0035g
- **Total mass** =19.964 + 11.85 + 13.0035 = 44.8175 g
- **Water** mass fraction=$\frac{19.964\ g}{44.8175g}$=.4455g
- **Acetone** mass fraction= $\frac{11.85\ g}{44.8175\ g}$ =.2644 g
- **Toluene** mass fraction= $\frac{13.0035\ g}{44.8175g}$ =.2901 g

➔ **Tie-line composition and othmer-Tobias Correlation (table 5)**

1- **Finding (a)value**

- **RI of water layer** =1.3540
- From calibration curve of RI (values from figure (4)), the **calibration equation** Y = 0.00065 X + 1.33520
- **Mass fraction of acetone** in water saturated with toluene.

  X = $(\frac{Y - 1.33520}{0.065})$ applying this $X = \left(\frac{1.3540-1.33520}{0.065}\right) = 0.2892$
- Since we need to find the weight fraction of the solvent in the extract phase:

  Mass fraction of water in water layer =1 - mass fraction of acetone

  =1 - 0.2892 = 0.7108

2- **Finding (b) value:**

- **RI of toluene** layer=1.4620
- From calibration curve of RI (values from figure (5), the **calibration equation**

Y = -0.00135 X + 1.49950

- **Mass fraction of acetone** in toluene saturated with water,

X = $(\frac{Y - 1.4995}{-0.135})$, applying this: X = $(\frac{1.4620-1.4995}{-0.135}) = 0.28$

- Since we need to find the weight fraction of the carrier liquid in the raffinate phase: **Mass fraction of toluene** in toluene layer =1 -mass fraction of acetone

= 1- 0.28 = 0.72

3- **Checking reliability by Othmer -Tobias correlation**

- The reliability of equilibrium data for any system may be tested by applying the Othmer- Tobias correlation:

$$\log\left(\frac{1-a}{a}\right) = n \log\left(\frac{1-b}{b}\right) + s$$

There is a linear relation between the values of $(\log(\frac{1-a}{a}))$and$(\log(\frac{1-b}{b}))$,where (a) represents water fraction in water layer, while (b) represents toluene fraction in toluene layer.

- As sample of calculation, x, and f(x) can be found as below:
  - ➔ X = $\log(\frac{1-b}{b}) = \log\left(\frac{1-0.7108}{0.7108}\right) = -0.3905$
  - ➔ F(X) = $\log(\frac{1-a}{a}) = \log\left(\frac{1-0.7222}{0.7222}\right) = -0.4150$

The same calculation has been applied on the other points and plotted to find the linear expression for the resulting line.

❖ Raw Data

Version no. 7 September, 2020

Liquid-Liquid Equilibrium Data Sheet

Tie-Lines Determination:

Volume of water (ml)	Volume of Toluene (ml)	Volume of Acetone (ml)	RI of water layer	RI of Toluene layer
1 20	15	15	1.3540	1.4620
18	20	13		
2 26	17	8	1.3365	1.4999
20	25	5		
3 19	29	3	1.3416	1.4942

Solubility curve

A. Water rich phase:

Volume of Acetone (ml)	Volume of water (ml)	Volume of Toluene (ml)
5	20	0.1
10	20	3.3
15	20	1.5
10	10	0.9
20	10	1.9
30	10	3.5

B. Organic solvent rich phase:

Volume of Acetone (ml)	Volume of Toluene (ml)	Volume of water (ml)
5	20	0.3
10	20	0.4
15	20	0.4
10	10	0.6
20	10	0.4
30	10	2.8

Instructor signature:

Date: 21/3/2023

Page 16 of 48

❖ Reference Graphs

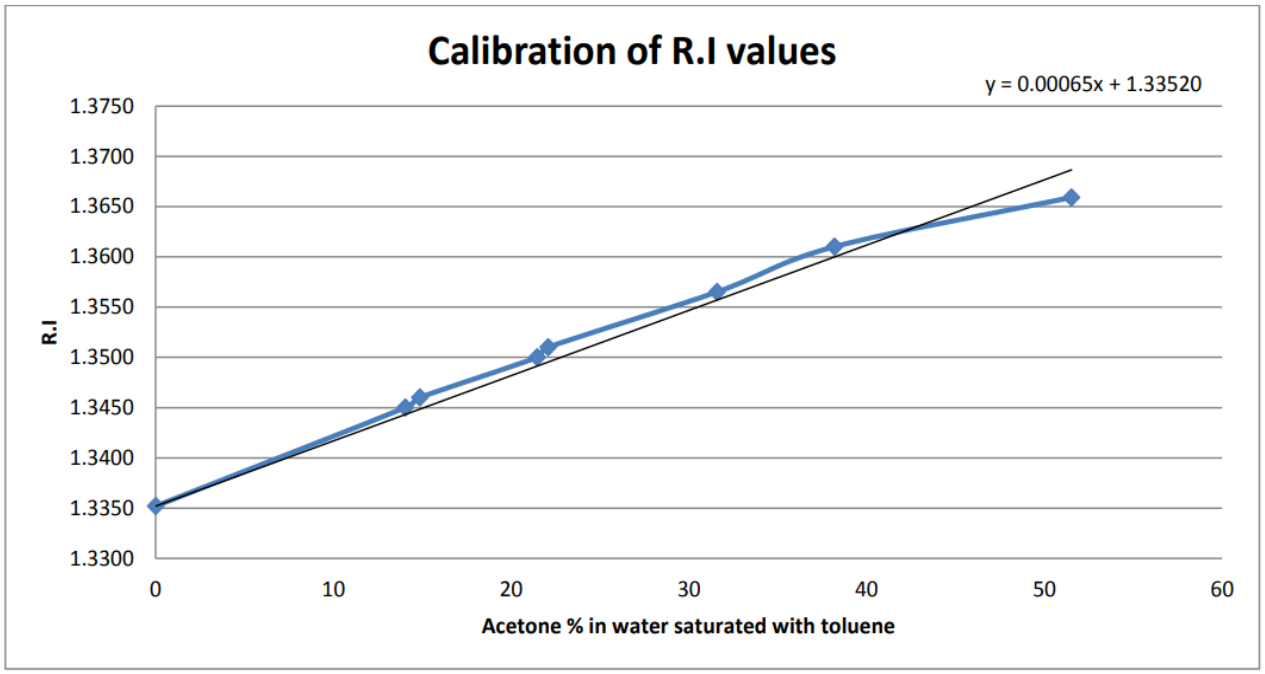

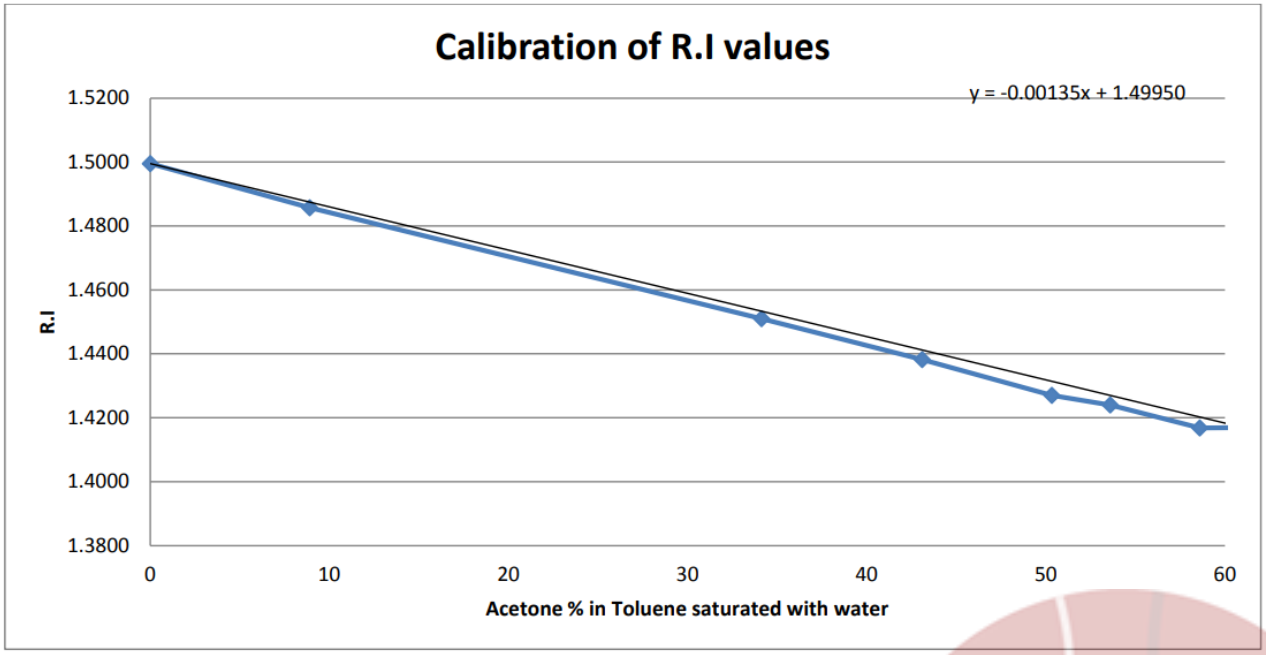

The University of Jordan

School of Engineering

Chemical Engineering Department

Chemical Engineering Laboratory (2) (0915461)

Experiment Number (3)

Digital Joulemeter

Type of the report: short report

Done by:

Instructor:

Eng. Rula Mohammad & Eng. Arwa Sandouqa

Performing Date: 09 / 05 / 2023

Submitting Date: 16 / 05 / 2023

Abstract

The Joulemeter measures power in watts and electrical energy directly in joules. It boasts a crystal-clear digital display that is very useful for demonstrations in class. It can be used to gauge the energy given to calorimeter heaters, as well as the power input to motors and output from dynamos, to determine how efficient they are. The goal of this experiment is to determine the specific heat capacity of aluminum, specific latent heat of Vaporization of water and to investigate the efficiency of a small electrical motor and study its variation with load and applied voltage. The Results show that the calculated heat capacity equal 1.1087 J/g.k which is different from the tabulated value due to weak insulation, calculated latent heat of vaporization equal 3046.6 J/g and the efficiency is increased with voltage increasing and decreased with mass increasing.

Table Of Contents

Table Of Figures

Table Of Tables

Results

Table 1 : Specific heat capacity experiment.

Mass of AL Block (g)	1011.98
Joule meter reading (J)	22440
T1 (ºC)	25
T2 (ºC)	45
Calculated Cp (J/g.k)	1.1087
True Cp of AL	0.902
Error (%)	**22.92**

Table 2 : Specific latent heat of vaporization experiment.

Mass Difference (Initial mass – Final mass) (g)	15.00
Temperature of liquid (ºC)	79
Temperature of liquid (K)	352.15
Joule meter reading (J)	45700
Calculated ΔHvap (J/g or KJ/Kg)	3046.67
True ΔHvap (J/g or KJ/Kg)	2308
Error (%)	32.00

Table 3 : Efficiency of a motor experiment at constant voltage (6 V)

At constant *voltage* (V) =	6		
Mass Lifted (without mass of the hanger) (g)	200	300	400
Mass Lifted (with mass of the hanger) (g)	220.23	320.23	420.23
Joulemeter Reading (input) (J)	3	6	16
Potential Energy (m × g × h) (output) (J)	1.080	1.571	2.061
Efficiency (η %)	36.008	26.179	12.883

Table 4 : Efficiency of a motor experiment at constant mass (200 g)

At constant *mass* (g) =	200		
Voltage (V)	5	6	7
Joulemeter Reading (input) (J)	7	3	2
Potential Energy (m × g × h) (output) (J)	1.080	1.080	1.080
Efficiency (η %)	15.432	36.008	54.011

Figures

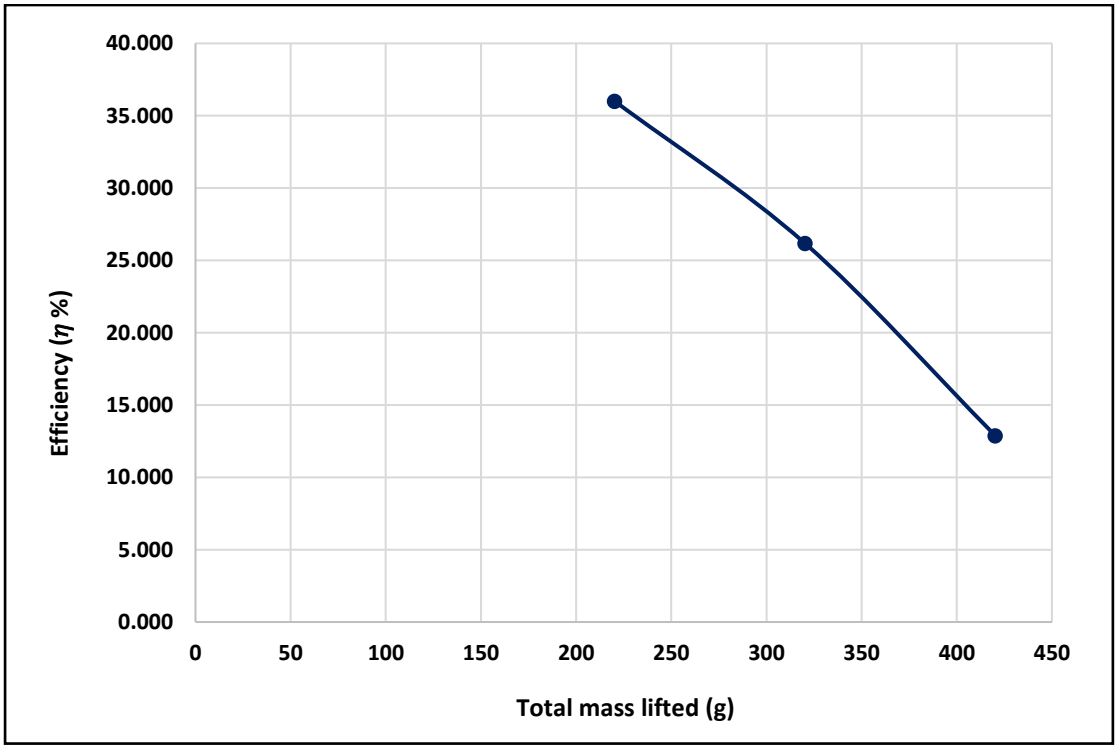

Figure 1 : Variation of efficiency with load at constant voltage (6 V).

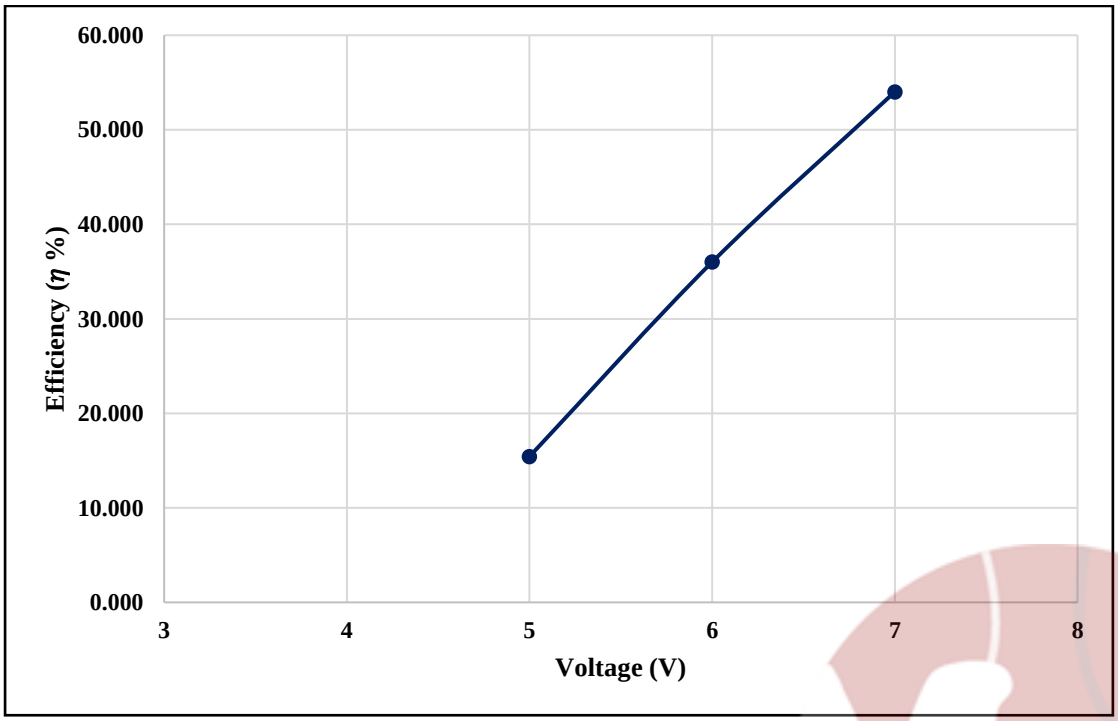

Figure 2: Variation of efficiency with load at constant mass (200 g).

Discussion

1) **In Specific heat capacity experiment**, as shown in table (1) we used the joulemeter as a source of heat, which transferred to the block of aluminum, the specific heat of the block is experimentally found to be 1.108718 (J/g.k) comparing this value to the true value which is equal to 0.902 (J/g.k). with a percentage error equal to 22.92% due to heat loss caused by the poor installation of the insulating material or the block was not 100% pure aluminum.

2) **In Specific latent heat of vaporization experiment**, as shown in table (2) we calculated the heat of vaporization of water at 79(ºC) and found to be 3046.67 J/g comparing this value to the true value found in tables such as (NIST values found in the appendix of most thermodynamics books such as Çengel:(Thermodynamics An Engineering Approach) which is equal to 2308 J/g with a percentage error equal to 32% which is relatively high might be caused by a false reading for the boiling point from the thermometer due to personal or systematic errors also could be caused by the impurities in water.

3) **In efficiency of a small electrical motor experiment**, in this part, the efficiency of the motor has been calculated by finding the ratio between the Electrical energy provided to the motor to the mechanical energy -which is the desired form of energy to be converted to according to the first law of thermodynamics, energy can neither be created nor destroyed, only altered in form. In the electric motor, part of the electric energy is converted to an unwanted form of energy such as heat or energy needed to resist friction.

   As shown in table (3) Increasing the mass increases the energy needed to move the weights, using more energy means more energy is lost during the process which explains decreasing the efficiency when increasing mass thus the efficiency is inversely proportional to mass as shown in figure (1).

   Also as shown in table (4) increasing the voltage while using fixed mass will increase the efficiency, thus the efficiency is directly proportional to voltage as shown in figure (2).

Conclusion

By conducting the experiment by digital Joulemeter to determine some properties in thermodynamics, we can conclude that:

1) **Specific heat capacity experiment**
   - Specific heat is the amount of heat required to raise the temperature of 1kg of a substance by 1°C and it can be found through the joule meter.
   - The amount of heat is directly proportional to the cp and a good isolation of the metal will increases the accuracy of the heat reading.
2) **Specific latent heat of vaporization experiment**
   - Latent heat of vaporization is the amount of heat that is required to evaporate 1 unit mass of a substance at constant temperature.
   - Increase in pressure leads to increases the boiling point of the liquid and a lesser amount of energy needed to overcome the intermolecular force thus the latent heat of steam required is decreased.
3) **Efficiency of a small electrical motor experiment**
   - The Joulemeter experiment proved to be an effective method for measuring the energy consumption of an electrical device.
   - By measuring the voltage and current in real-time, the Joulemeter was able to accurately calculate the energy usage and display it in various units, Voltage and the efficiency of the power source are inversely connected, the efficiency decline at constant voltage 6 V as the total mass lifted increased.
   - Variable voltage and constant mass; as the voltage rises, the motor's efficiency grows (direct relationship).
   - More energy is needed to move the weights as mass increases.

References

1) Chemical engineering laboratory "2" (0915461); University of Jordan; faculty of engineering and Technology; Department of Chemical engineering.

2) YUNUS A. ÇENGEL, MICHAEL A. BOLES, MEHMET KANOĞLU, (2019), "Thermodynamics, An Engineering Approach", 9th edition, McGraw-Hill Education.

Appendix

❖ Sample of calculation:

➢ Experiment 1: Determination of the specific of heat capacity of metal:

- Mass of (AI) block = 1011.98 g
- Joule meter reading (Q) = 22440 J
- Initial temperature (T_1) = 25 **ºC**
- Final temperature (T_2) = 45 **ºC**
- Temperature difference (ΔT) =$T_2 - T_1$ = 45 - 25= 20 K
- $Q = m \times Cp \times \Delta T$
- $Cp = \frac{Q}{m \times \Delta T} = \frac{22440\ J}{1011.98\ g \times 20K}$ =1.108 J/g.k
- True Cp of AL= 0.902 J/g.k
- **Error** = $\left(\frac{1.108 - 0.902}{0.902}\right) \times 100\%$ = **22.92 %**

➢ Experiment 2: Determination of the specific latent heat of vaporization of liquids.

- Change in mass of liquid = 15 g
- Temperature of liquid = 79 ℃
- Joule meter reading (J) = 45700 J
- Mass of vaporized water =15 g
- Latent heat of Vaporization (ΔH_{vap}) = $\frac{Q}{m} = \frac{45700}{15}$ = 3046.67 J/g
- True ΔH_{vap} = 2308 J/g
- **Error** = $\left(\frac{3046.67 - 2308}{2308}\right) \times 100\ \% = \mathbf{32\%}$

- **Experiment 3: Efficiency of a small electrical motor**

➔ **At constant voltage = 6 V**

- Change in height = 50 Cm
- Mass of hanger = 20.23 g
- Mass added = 200 g
- Total mass = 200 + 20.32 = 220.32 g = 0.22032 kg
- Joule meter reading = 3 J (input energy)
- Potential energy = m × g × Δh (output energy)

  Potential energy = $0.22032\ Kg \times 9.81 \frac{m}{s^2} \times 50 \times 10^{-2}$ m = 1.080 J
- Efficiency = $\frac{\text{output energy}}{\text{input energy}}$

  Efficiency = $(\frac{1.080J}{3J}) \times 100\ \% = 36.008\%$

➔ **At constant mass = 200 g**

- Mass of hanger = 20.23 g
- Total mass = 220.23 g
- Change in height = 50 cm
- Voltage = 5 V
- Joule meter reading = 7J
- Potential energy = $(\frac{220.23}{1000})Kg \times 9.81\ \frac{m}{s^2} \times 50 \times 10^{-2}$ m = 1.080 J
- Efficiency = $\frac{\text{output energy}}{\text{input energy}}$

  Efficiency = $\left(\frac{1.080\ J}{7\ J}\right) \times 100\% = 15.43\%$

Version no. 7 September, 2020

Digital Joulemeter Data Sheet

1. Specific heat Capacity:

Mass of AL-Block	1011.989
Joule meter reading	2244 x10
T_1	25
T_2	45

2. Specific latent heat of vaporization:

Initial mass of liquid	÷15.00
Final mass of liquid	
Temperature of liquid	79
Joule meter reading	4570 x10

3. Efficiency of a motor:

Change in height=……50……cm

Mass of hanger=……~~200~~……g

20.23

a. At constant Voltage=……6……V

Mass lifted (g)	Joule meter reading
200	3
300	6
400	16

a. At constant mass=…200…g

Voltage (V)	Joule meter reading
5	7
6	3
7	2

Instructor signature:

Date: 9/5/2023

The University of Jordan

School of Engineering

Chemical Engineering Department

Chemical Engineering Laboratory (2) (0915461)

Experiment Number (4)

Mixing of powder

Type of the report: short report

Done by:

Instructor:

Eng. Rula Mohammad

Performing Date: 14 / 03 / 2023

Submitting Date: 21 / 03 / 2023

Abstract

In industrial process engineering, mixing is a unit operation that obtained a homogeneous mixture in terms of concentration, density and particle size distribution. In this experiment, sand and salt (KCl) were mixed using a double cone mixer, the samples were taken at various times from the Top, Bottom, and Middle then was analyzed using titration with ($AgNO_3$) and the particle size, weight, mixing time and speed were considered.

The main objectives were to study the process of mixing and see how the properties of ingredients - the particle size distribution as example - will affect the process. Also investigate the effect of mixing time, and mixing speed on the state of mixing. The results show that the degree of mixing is maximum at t = 20 minutes, and the highest index was (0.181).

Table Of Contents

Table Of Figures

Table Of Tables

Results

Table 1 : Data and properties for calculations

	KCL	Sand
Particle size (µm)	675	275
Density (g/cm^3)	1.98	1.602
Particle volume (cm^3)	1.61E-04	1.09E-05
Mass of particle (g/particle)	3.19E-04	1.75E-05
Weight (g)	200.152	200.042
Number of particles	6.27E+05	1.15E+07
Total number of particles	1.21 E+07	
μ_p	0.0519	0.9481

Table 2 : Results at t= 5 mins

Location	Total weight (g)	V $AgNO_3$ (ml)	Moles $AgNO_3$	Moles of KCl	Mass of KCL	Mass of sand	X (KCL)	X (sand)	X (avg)	X - X_{avg}	$(X - X_{avg})^2$
Top	0.122	36.3	0.00363	0.00363	0.2706	-0.1486	2.218	-1.218	-0.856	-0.3619	0.1310
Bottom	0.106	33.7	0.00337	0.00337	0.2512	-0.1452	2.370	-1.370		-0.5138	0.2640
Middle	0.111	14.6	0.00146	0.00146	0.1088	0.002156	0.981	0.0194		0.8757	0.7669
										SUM	1.1619

Table 3 : Results at t= 10 mins

Location	Total weight (g)	V $AgNO_3$ (ml)	Moles $AgNO_3$	Moles of KCl	Mass of KCL	Mass of sand	X (KCL)	X (sand)	X (avg)	X - X_{avg}	$(X - X_{avg})^2$
Top	0.1	6.9	0.00069	0.00069	0.0514	0.0486	0.5144	0.4856	0.476	0.0096	0.0001
Bottom	0.112	10.4	0.00104	0.00104	0.0775	0.0345	0.6922	0.3077		-0.1683	0.0283
Middle	0.1	4.9	0.00049	0.00049	0.0365	0.0635	0.3653	0.6347		0.1587	0.0252
										SUM	0.05359

Table 4 : Results at t= 15 mins

Location	Total weight (g)	V $AgNO_3$ (ml)	Moles $AgNO_3$	Moles of KCl	Mass of KCL	Mass of sand	X (KCL)	X (sand)	X (avg)	X - X_{avg}	$(X - X_{avg})^2$
Top	0.1	14.6	0.00146	0.00146	0.1088	-0.0088	1.0884	-0.088	0.25035	-0.3388	0.1148
Bottom	0.1	8.9	0.00089	0.00089	0.0664	0.0336	0.6635	0.3365		0.0861	0.0074
Middle	0.105	7	0.0007	0.0007	0.0522	0.0528	0.4970	0.5030		0.2526	0.0638
										SUM	0.186

Table 5: Results at t= 20 mins

Location	Total weight (g)	V $AgNO_3$ (ml)	Moles $AgNO_3$	Moles of KCl	Mass of KCL	Mass of sand	X (KCL)	X (sand)	X (avg)	X - X_{avg}	$(X - X_{avg})^2$
Top	0.1	10	0.001	0.001	0.0746	0.0254	0.7455	0.2545	0.2229	0.0316	0.00100
Bottom	0.1	10.8	0.00108	0.00108	0.0805	0.0195	0.8052	0.1948		-0.0280	0.00079
Middle	0.106	11.1	0.00111	0.00111	0.0828	0.0232	0.7807	0.2193		-0.0036	0.00001
										SUM	0.008

Table 6: Results at t= 30 mins

Location	Total weight (g)	V $AgNO_3$ (ml)	Moles $AgNO_3$	Moles of KCl	Mass of KCL	Mass of sand	X (KCL)	X (sand)	X (avg)	X - X_{avg}	$(X - X_{avg})^2$
Top	0.102	35.3	0.00353	0.00353	0.2632	-0.1612	2.5800	-1.5800	-0.805	-0.7754	0.6013
Bottom	0.104	20.5	0.00205	0.00205	0.1528	-0.0488	1.4695	-0.4695		0.3351	0.1123
Middle	0.1	18.3	0.00183	0.00183	0.1364	-0.0364	1.3643	-0.3643		0.4403	0.1939
										SUM	0.9075

Table 7: Results at t= 45 mins

Location	Total weight (g)	V $AgNO_3$ (ml)	Moles $AgNO_3$	Moles of KCl	Mass of KCL	Mass of sand	X (KCL)	X (sand)	X (avg)	X - X_{avg}	$(X - X_{avg})^2$
Top	0.1	37.7	0.00377	0.00377	0.2811	-0.1811	2.8106	-1.8106	-1.057	-0.7537	0.5681
Bottom	0.1	39.3	0.00393	0.00393	0.2930	-0.1930	2.9299	-1.9299		-0.8730	0.7621
Middle	0.104	6	0.0006	0.0006	0.0447	0.0593	0.4301	0.5699		1.6267	2.6463
										SUM	3.9765

Table 8: Results at t= 60 mins

Location	Total weight (g)	V $AgNO_3$ (ml)	Moles $AgNO_3$	Moles of KCl	Mass of KCL	Mass of sand	X (KCL)	X (sand)	X (avg)	X - X_{avg}	$(X - X_{avg})^2$
Top	0.1	17.4	0.00174	0.00174	0.1297	-0.0297	1.2972	-0.2972	-0.672	0.3752	0.1408
Bottom	0.1	20.7	0.00207	0.00207	0.1543	-0.0543	1.5432	-0.5432		0.1292	0.0167
Middle	0.1	29.2	0.00292	0.00292	0.2177	-0.1177	2.1769	-1.1769		-0.5045	0.2545
										SUM	0.4120

Table 9: Results of mixing index during mixing

At t =		5 mins	10 mins	15 mins	20 mins	30 mins	45 mins	60 mins
Number of salt particle during mixing	**Top**	848.4	161.3	341.2	233.7	825.0	881.1	406.7
	Middle	787.7	243.1	208.0	252.4	479.1	918.5	483.8
	Bottom	341.2	114.5	163.6	259.4	427.7	140.2	682.5
Number of sand particle during mixing	**Top**	8516.2	2782.6	506.8	1458.3	9235.0	10374.9	1702.9
	Middle	8322.3	1975.0	1928.2	1116.5	2798.0	11058.4	3112.7
	Bottom	123.5	3636.9	3026.3	1332.2	2087.4	3396.2	6743.8
	SUM	16962.0	8394.5	5461.3	3906.9	14120.4	24829.4	11559.3
Index		2.23E-03	1.48E-02	9.84E-03	1.18E-01	2.77E-03	9.98E-04	4.55E-03

Figures

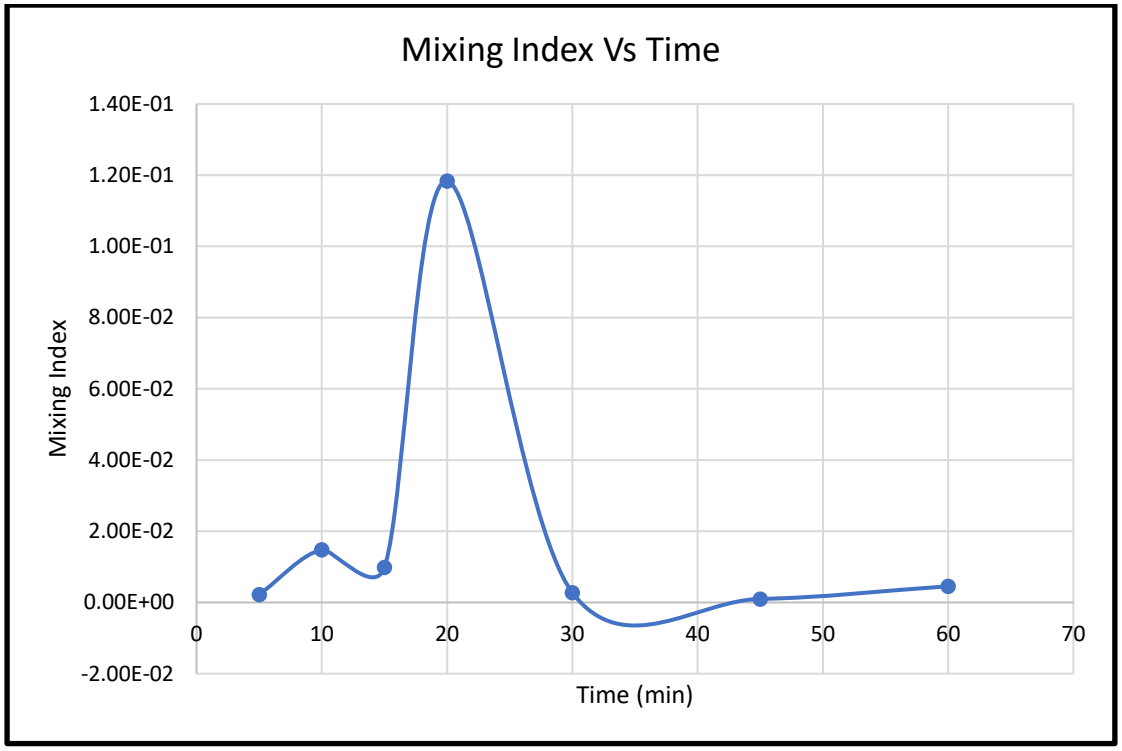

Figure 1 : Mixing Index Vs Time.

Discussion

Mixing of granular materials is unquestionably important. Mixing solids is common in industrial applications and frequently represents a critical stage of the processes. The effect of mixing determines the quality of products, Index of mixing is an indicator of the quality of the mixing process and was used to determine the effect of mixing time on the homogeneity of the multi-component granular mixtures(salt and sand in this experiment)

As shown in (Figure 1) it cannot be clearly said that as the mixing time increases, the homogeneity of the granular mixture increases, The optimum mixing was at 20 min and the highest

index was (0.181), affected by many factors such as particle size as shown in (Table 1) the larger the particle size of the powder, the more coarse the powder, the lower the tendency of the powder to mix when mixing.

On the other hand, when ρ is decreased, the weight of large particles become dominant, and large particles would be able to overcome the upward forces on them to move into small particle region at the bottom.

Personal error might have occurred due to inaccurate reading of volume measurements from the burette. Instrumental error might have played a role as well in the losses of particles found in the double cone mixer.

Conclusion

By conducting the experiment at different time intervals, we can conclude that:

- The mixing index is measure of the homogeneity of mixture and how far mixing has produced toward equilibrium. In this experiment the mixing index have the higher value at 20 min, so it is the best time of mixing.
- The mixing time is a factor effect on mixing and optimum time should be defined, the best time of mixing is not determined by the longest time.
- Increase the spot sample makes the result more accurate.
- The electrostatic force repulsion causes the mixing to achieve a maximum value at the optimal mixing period, and then it lowers as a result of the electrostatic force repulsion.
- The rate of mixing as measured by the rate of change of Is with time, varies greatly with kind of mixers and the properties of mixed material, such as particles size, solids of different particle Sizes have the tendency to separate again after certain time of mixing, with the small particles in one area and the big ones in another area.

References

1) Chemical engineering laboratory “2” (0915461); University of Jordan; faculty of engineering and Technology; Department of Chemical engineering.
2) Coulson and Richardson, (2019)," Chemical Engineering " Vol.II , 6th edition, Pergamon Press

Appendix

- **Sample of calculation:**
  - **From Table 1:**
    1. **d_{avg}**
       - ➔ $d_{avg\,,\,KCl} = \frac{500 + 850}{2} = 675$
       - ➔ $d_{avg\,,\,sand} = \frac{200 + 350}{2} = 275$
    2. **Particle volume**
       - ➔ $V_{KCl} = \frac{\pi\, d^3_{avg,KCl}}{6} = 1.61 \times 10^{-4}\ cm^3$
       - ➔ $V_{sand} = \frac{\pi\, d^3_{avg,sand}}{6} = 1.09 \times 10^{-5}\ cm^3$
    3. **Mass of particle**
       - $\rho_{KCl} = 1.98\ g/cm^3$, $\rho_{sand} = 1.602\ g/cm^3$
       - ➔ $m_{KCl} = \rho_{KCl} \times V_{KCl} = 3.19 \times 10^{-4}$ g / particle
       - ➔ $m_{sand} = \rho_{sand} \times V_{sand} = 1.75 \times 10^{-5}$ g / particle
    4. **Number of particles**
       - $W_{KCl} = 200.152$ g , $W_{sand} = 200.042\ g/cm^3$
       - ➔ $n_{KCl} = \frac{W_{KCl}}{m_{KCl}} = 6.27 \times 10^{+5}$ particles
       - ➔ $n_{sand} = \frac{W_{sand}}{m_{sand}} = 1.15 \times 10^{+7}$ particles
       - ➔ **Total number of particles =** $n_{KCl} + n_{sand} = 1.21 \times 10^{+7}$
    5. **μ_p**
       - ➔ **For salt:** $(1 - \mu_p) = \frac{n_{KCl}}{\text{Total number of particles}} = 0.0519$
       - ➔ **For sand:** $\mu_p = \frac{n_{sand}}{\text{Total number of particles}} = 0.9481$
  - **From Table 2; taking the 1st row:**
    1. **Number of spot samples:**
       - ➔ **N =** 3 (Top, Middle, Bottom)
    2. **Volume of $AgNO_3$:**
       - ➔ $V = V_F - V_i = 36.3 \pm 0.07\ cm^3$
       - ➔ **Error =** $\sqrt{0.5^2 + 0.5^2} = 0.07$ (uncertainty of the burette due to the difference of volume reading).

3. **Moles of $AgNO_3$:**

   ➔ $[\mathbf{AgNO_3}]$ = 0.1 M

   ➔ **Mol.es of $AgNO_3$** = $[AgNO_3] \times V$ = 0.1 × 36.3 = 0.00363 mole

4. **Moles of KCl**

   ➔ **Moles of KCl** = Moles of $AgNO_3$ = 0.00363 mole

5. **Mass of KCl**

   ➔ KCl molar mass =74.55 g/mol

   ➔ Mass of KCl = Mole of KCl × Mw = 0.2706 g

6. **Mass of sand**

   ➔ **Mass of sand** = Sample wight – mass of KCl = 0.122 – 0.2706 = -0.1486 !!

7. **Mass fraction of silica sand and salt (X_{salt} , X_{sand})**

   ➔ $\mathbf{X_{salt}} = \frac{\text{Mass of KCl}}{\text{Sample wight}} = \frac{0.2706}{0.122}$ = 2.2182 !!

   ➔ $\mathbf{X_{sand}} = \frac{\text{Mass of sand}}{\text{Sample wight}} = \frac{-0.1486}{0.122}$ = -1.2182 !!

   ➔ Mass fraction of sand for other two spots are: -1.03702, 0.01942

8. **The average of mass fraction of sand:**

   ➔ $\mathbf{X_{avg}} = \frac{-1.2182 + -1.03702 + 0.01942}{3}$ = -0.85631

➢ **From Table 9:**

1. **Number of sand and salt particles during mixing**

   ➔ **For salt: n =** $\frac{\text{weight of salt}}{\text{mass of salt particle}} = \frac{0.2706}{3.19 \times 10^{-4}}$ = 848.4 particles

   ➔ **For sand: n =** $\frac{\text{weight of sand}}{\text{mass of sand particle}} = \frac{0.1486}{1.75 \times 10^{-5}}$ = 8516.2 particles

   ➔ **n for sand in the two other spots:** 8322.3, 123.5

   ➔ $\sum$ **n** = 8516.2 + 8322.3 + 123.5 = 16962 particles

2. **The Index of mixing in each interval of time according to this equation:**

$$I_s = \sqrt{\frac{\mu_p \cdot (1 - \mu_p) \cdot (N - 1)}{n \cdot \sum_{i=1}^{n} (x_i - x_{avg})^2}}$$

   ➔ $I_s = \sqrt{\frac{0.0519 \times 0.9481 \times (3-1)}{16962 \times 1.1619}}$ = 2.23 E -03

Version no. 7 September, 2020

Mixing of Powder Data Sheet

Weight of salt: 201.152 g Particle size of salt: 675

Weight of sand: 200.042 g Particle size of sand: 425

Time	Sample Location	Sample wt(g)	Vol. of $AgNO_3$ (ml)
5 min	Top	0.122	36.3
	Bottom	0.106	33.7
	Right (mid)	0.111	14.6
	Left		
10 min	Top	0.100	6.9
	Bottom	0.112	10.4
	Right (mid)	0.100	4.9
	Left		
15 min	Top	0.100	14.6
	Bottom	0.100	8.9
	Right (mid)	0.105	7.0
	Left		
20 min	Top	0.100	10.0
	Bottom	0.100	10.8
	Right (mid)	0.106	11.1
	Left		
30 min	Top	0.102	35.3
	Bottom	0.104	20.5
	Right (mid)	0.100	18.3
	Left		
45 min	Top	0.100	37.7
	Bottom	0.100	39.3
	Right (mid)	0.104	6.0
	Left		
60 min	Top	0.100	17.4
	Bottom	0.100	20.7
	Right (mid)	0.100	29.2
	Left		

Instructor signature:

Date: 14/3/2023

Page 25 of 48

The University of Jordan

School of Engineering

Chemical Engineering Department

Chemical Engineering Laboratory (2) (0915461)

Experiment Number 5

Fluidized Bed Heat Transfer Unit

Type of the report: short report

Done by:

Instructor:

Eng. Rula Mohammad

Performing Date: 2/ 05 / 2023

Submitting Date: 9 / 05 / 2023

Abstract

A fluidized bed is a physical phenomenon that occurs when a solid particulate substance (usually present in a holding vessel) is under the right conditions so that it behaves like a fluid. The usual way to achieve a fluidized bed is to pump pressurized fluid into the particles. The resulting medium then has many properties and characteristics of normal fluids, such as the ability to free-flow under gravity, or to be pumped using fluid technologies, the resulting phenomenon is called fluidization. In this experiment, the main objectives were to show the effect of fluid velocity on pressure drop through the fluidized bed. The results show that the pressure drop increase as the flow rate increase and after fludization the pressure drop will be constant.

Table of Contents

Table of Figure

Table of Tables

Result

Table 1: Effect of the variation in flow rate on the pressure drop (for low flow rate)

Flow rate	Actual flow rate	Δp (cmH_2O)	Observation
1	3	3.9	Static
2	4	4.2	Static
3	5	4.8	Slightly static
4	6	5.4	Slightly static
5	7	5.7	Slightly static
6	8	5.9	Slightly static
7	9	6	Moving
8	10	6.1	Moving
9	11	6.2	Moving
10	12	6.3	Moving
11	13	6.5	Moving
12	14	6.6	Bubbles
13	15	6.7	Bubbles
14	16	7.1	Bubbles
15	17	7.2	Bubbles
16	18	7.3	More bubbles
17	19	7.4	Big bubble
18	20	7.45	Big bubble
19	21	7.5	Big bubble
20	22	7.7	Turbulent
21	23	7.8	Turbulent
22	24	7.9	Turbulent

Table 2: Effect of the variation in flow rate on the pressure drop (for high flow rate)

Flow rate	Actual flow rate	Δp (cmH_2O)	Observation
2	45	8.1	More bubbles
3	48	8.9	More bubbles
4	49	9.5	More bubbles
5	50	10	Big bubble
6	55	11	Big bubble
7	60	11.8	Big bubble
8	65	12.7	Turbulent
9	70	13.6	Turbulent
10	75	14.7	Turbulent
11	80	15.8	More turbulent
12	85	16.8	More turbulent

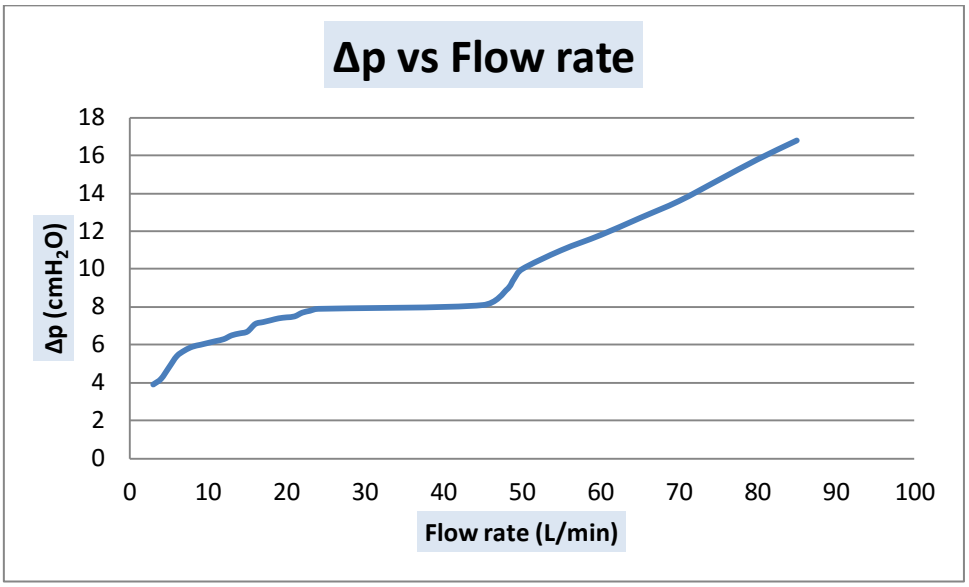

Figure 1: Δp (cmH2O) vs Flow rate(L/min)

Discussion

The speed of the air flow affects how much pressure drops inside the bed. as observed. The relationship between air flow and pressure can be shown by comparing Tables (1) and (2). The incremental flow rate fluctuation on Figure 1 is depicted.

Little bubbles first started to emerge on the material's surface inside the bed as a result of the pressure drop caused by the increased air flow, and they moved up the material from the bottom to the top. When the air flow speed is greatly increased, big air bubbles start to appear. These air bubbles might travel further into the material bed and help to mix it.

Because the pressure in the bed is inversely related to the centrifugal weight of the bed, the pressure drop rises as the flow rate increases as expected. The ideal value of pressure drop is unknown due to experimental constraints (not covering the entire range of flow rate).

Conclusion

By conducting the experiment at different air flow rates, we can conclude that:

* As the value of the air flow rate increases, the mixing between the particles increases and the porosity of the bed increases.

* The pressure drop is directly proportional with fluid flow rate.

* At low flow rate the bed is stationary, and at high flow rate the particles start moving and individual particle separate from each other, then the bed is called fluidized Bed when the fluid reach the minimum fluidization velocity.

* As the air flow rate is increased, the input power value which equals (V.I) will also increase.

* The heat transfer coefficient is directly proportional with fluid velocity.

References

1) Chemical engineering laboratory “2” (0915461); University of Jordan; faculty of engineering and Technology; Department of Chemical engineering.

Appendix

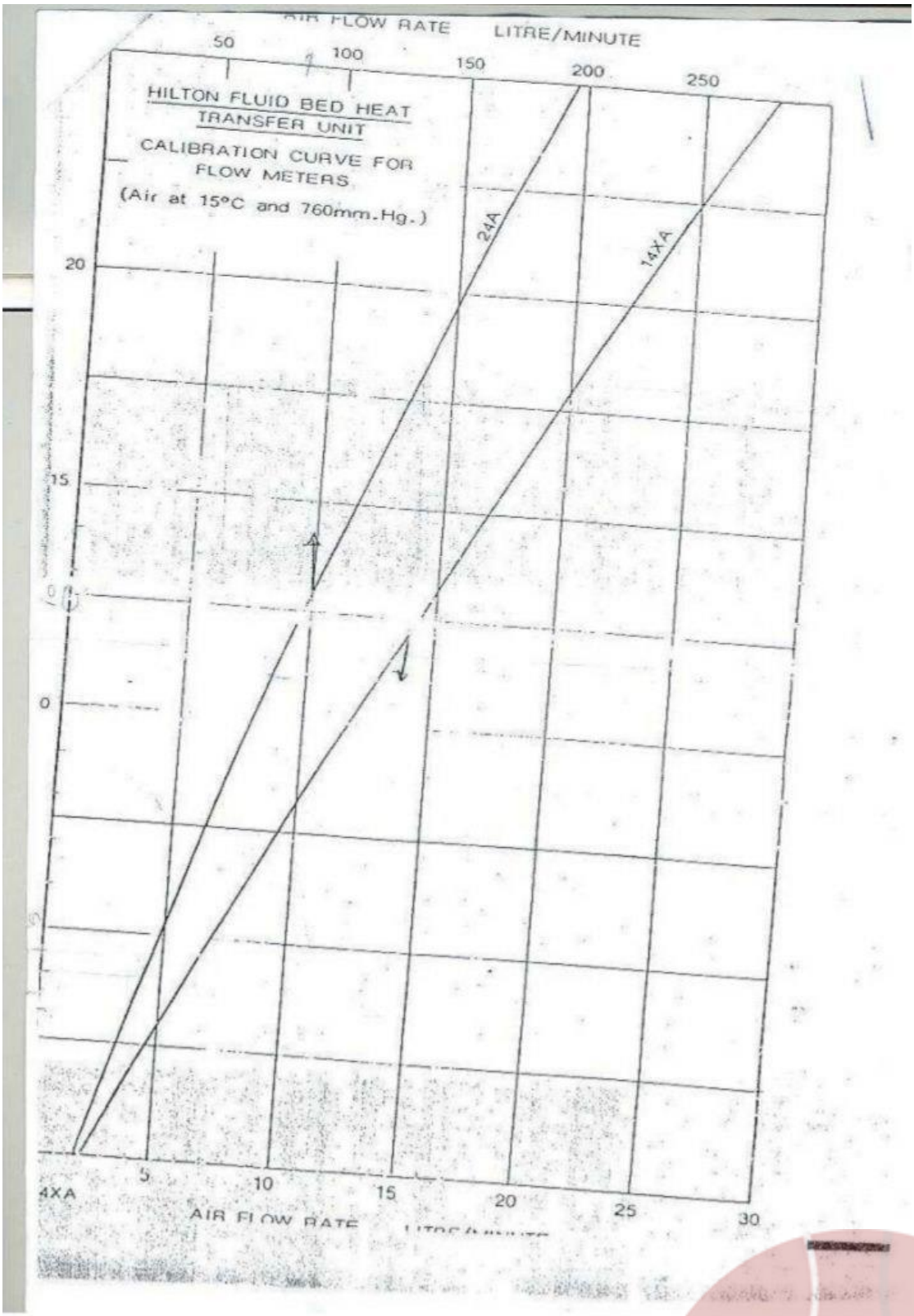

Figure 2: Calibration curve for flow meters for fluid bed heat transfer unit

Version no. 7 September, 2020

Fluidized Bed Heat Transfer Unit Data Sheet

Flow rate	~~T_1 (°C) Bed Temp.~~ F	T_2 (°C) Heater Temp.	T_3 (°C) Air Temp.	ΔP ~~Voltage (V)~~	~~Current (A)~~	ΔP(cmH_2O) -2	Observation
1	2			8.1	8	3.9	Static
2	3			8.9		4.2	Static
3	4			9.5		4.8	slightly static
4	5			10		5.4	slightly static
5	6			11		5.7	" "
6	7			11.8		5.9	" "
7	8			12.7		6	Moving
8	9			13.6		6.1	Moving
9	10			14.7	بلمميزة	6.2	"
10	11			15.8	More	6.3	"
11	12			16.8	turbulence	6.5	"
12	~~13~~					6.6	bubble
13	~~14~~					6.7	"
14						7.1	"
15						7.2	"
16						7.3	More bubble
17						7.4	Big bubble
18						7.45	" "
19						7.5	" "
20						7.7	Turbulence
21						7.8	"
22						7.9	"

Instructor signature: Rula Mustafa 21/5/2023

Date: 21/5/2023.

Page 29 of 48

1-22 low flow rate.
high flow rate

The University of Jordan

School of Engineering

Chemical Engineering Department

Chemical Engineering Laboratory (2) (0915461)

Experiment Number (6)

Jaw Crusher

Type of the report: short report

Done by:

Instructor:

Eng. Rula Mohammad

Performing Date: 28 / 03 / 2023

Submitting Date: 4 / 04 / 2023

Abstract

Crushing is the process of reducing a material's size so that it can be treated further. Industrial crushing equipment can be highly helpful in a wide range of enterprises in addition to the chemical industry. This experiment's goal is to investigate the comminution behavior of various materials using a primary crusher (a jaw crusher) in a variety of conditions while taking power requirements into account. The result showed that the coarse particle had the greatest amount of power required.

Table of Contents

Table of Figures

Table of Tables

Results

❖ Coarse particles

Table 1: Properties for crushing coarse size particles and power required.

Coarse size						
Dimension of feed particle's	**Length (cm)**	**Width (cm)**	**Hight (cm)**	**Volume (cm^3)**	**dv (mm)**	**d_{80} (mm)**
	3	2	0.8	4.8	17.88	1.29
	1.5	2	1	3		
	2.5	2	0.5	2.5		
	3	1.4	0.4	1.68		
Weight of sample	350.8g=0.00035 ton					
Time needed for crushing	43.22sec=0.01201 hr					
Feed flow rate (ton /hr)	0.02914238					
Power (Kw)	0.063404177					

$V_{avg} = 2.995\ cm^3$

Table 2: Cumulative distribution for coarse size

Corse particles				
Sieve size	**davg(mm)**	**Weight (g)**	**Weight (%)**	**Weight cumulative (%)**
x > 1.4 mm	1.4	82.5	26.85	100
1.4mm>x>1mm	1.2	57.6	18.75	73.14
1 mm>x>850µ	0.9250	17.5	5.69	54.39
850µm>x > 500µm	0.6750	47	15.29	48.69
500µm> x >355µm	0.42750	23.3	7.58	33.39
355µm> x > 250µm	0.30250	17.5	5.69	25.81
250 µm> x > 125µm	0.18750	21.5	6.99	20.11
125µm>x>90µm	0.10750	16.1	5.24	13.11
x<90µm	0.090	24.2	7.87	7.87
Total		307.2		

❖ Intermediate Particles

Table 3: Properties for crushing intermediate size particles and power required.

Intermediate size						
Dimension of feed particle's	**Length (cm)**	**Width (cm)**	**Hight (cm)**	**Volume (cm3)**	**d_v (mm)**	**d_{80} (mm)**
	2	1.5	0.4	1.2	12.47	1.24
	2.7	1.5	0.4	1.62		
	1.8	1.1	0.5	0.99		
	2.5	1	0.1	0.25		
Weight of sample	350.5 g =0.000351 ton					
Time needed for crushing	52.19 sec=0.014497 hr					
Feed flow rate (ton / hr)	0.024177045					
Power (Kw)	0.064033801					

$$V_{avg} = 1.015\ cm^3$$

Table 4: Cumulative distribution for intermediate size.

Intermediate particle				
Sieve size	**davg(mm)**	**Weight (g)**	**Weight (%)**	**Weight cumulative (%)**
x > 1.4 mm	1.4	81.7	23.87	100
1.4mm>x>1mm	1.2	68.7	20.07	76.12
1 mm>x>850µm	0.9250	24.3	7.10	56.049
850µm>x > 500µm	0.6750	55.3	16.16	48.94
500µm> x >355µm	0.42750	28.7	8.38	32.78
355µm> x > 250µm	0.3025	21.3	6.22	24.40
250 µm> x > 125µm	0.18750	25.4	7.42	18.17
125µm>x>90µm	0.10750	10.2	2.98	10.75
x<90µm	0.090	26.6	7.77	7.77
Total		342.2		

❖ Fine Particles

Table 5: Properties for crushing fine size particles and power required.

Fine size						
Dimension of feed particle's	**Length (cm)**	**Width (cm)**	**Hight (cm)**	**Volume (cm3)**	**d_v (mm)**	**d_{80} (mm)**
	1	0.7	0.1	0.07		1.2
	0.6	0.3	0.7	0.126		
	1.2	0.5	0.4	0.24		
	0.9	0.3	0.1	0.027	6.05	
Weight of sample	350 g=0.00035 ton					
Time needed for crushing	1.07 min=0.017833 hr					
Feed flow rate (ton / hr)	0.019626					
Power (Kw)	0.054423713					

V_{avg}=0.11575 cm^3

Table 6: Cumulative distribution for fine size.

Fine particle				
Sieve size	**d_{avg}(g)**	**Weight (g)**	**Weight (%)**	**Weight cumulative (%)**
x > 1.4 mm	1.4	60	17.59	100
1.4mm>x>1mm	1.2	67.2	19.70	82.40
1 mm>x>850µ	0.9250	27.1	7.94	62.70
850µm>x > 500µm	0.6750	65.5	19.20	54.76
500µm> x >355µm	0.42750	29.7	8.70	35.56
355µm> x > 250µm	0.30250	23	6.74	26.85
250 µm> x > 125µm	0.18750	28.1	8.23	20.11
125µm>x>90µm	0.10750	10.8	3.16	11.87
x<90µm	0.090	29.7	8.70	8.70
Total		341.1		

Table 7: Different particles size of product and feed and power required for crushing.

	Weight of sample (ton)	**Time need for crushing (hr)**	**Feed flow rate (ton/hr)**	**Feed Particle size L1 (mm)**	**Feed Particle size L2 (mm)**	**Work index (kw.hr /ton)**	**Power (KW)**
Coarse size	.000350	0.012010	0.002914	25	1.29	15.8	0.0634
Intermediate size	0.00351	0.0144970	0.024177	22.5	1.24	15.8	0.0640
Fine size	0.000350	0.0178330	0.019626	9.25	1.2	15.8	0.0544

Figures

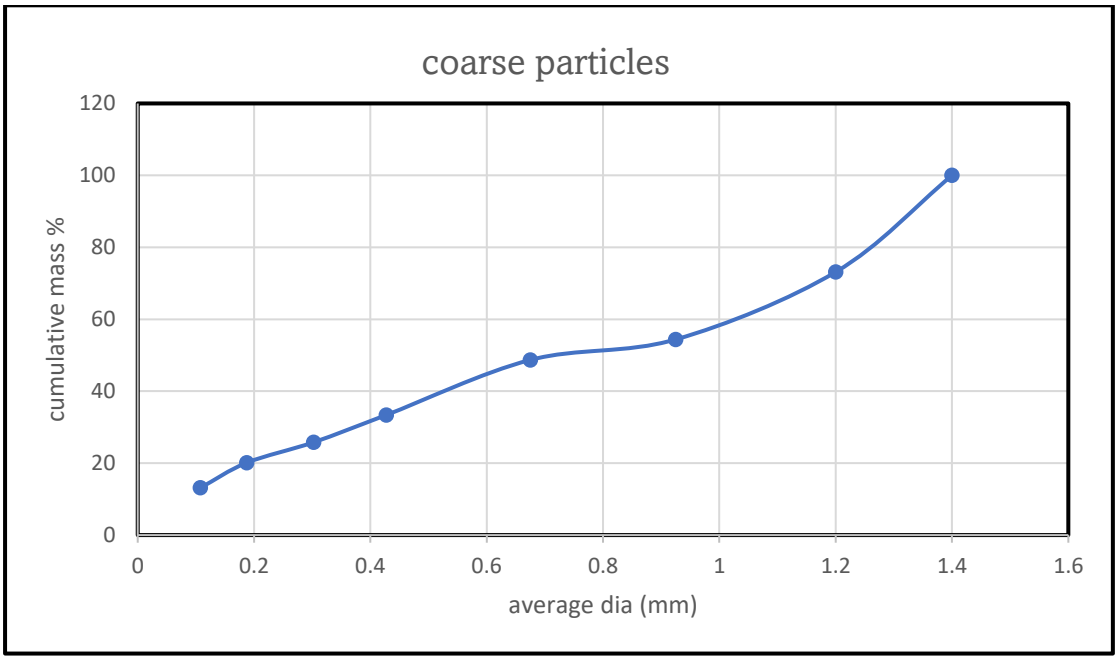

Figure 1: Accumulative mass percent average diameter for coarse size

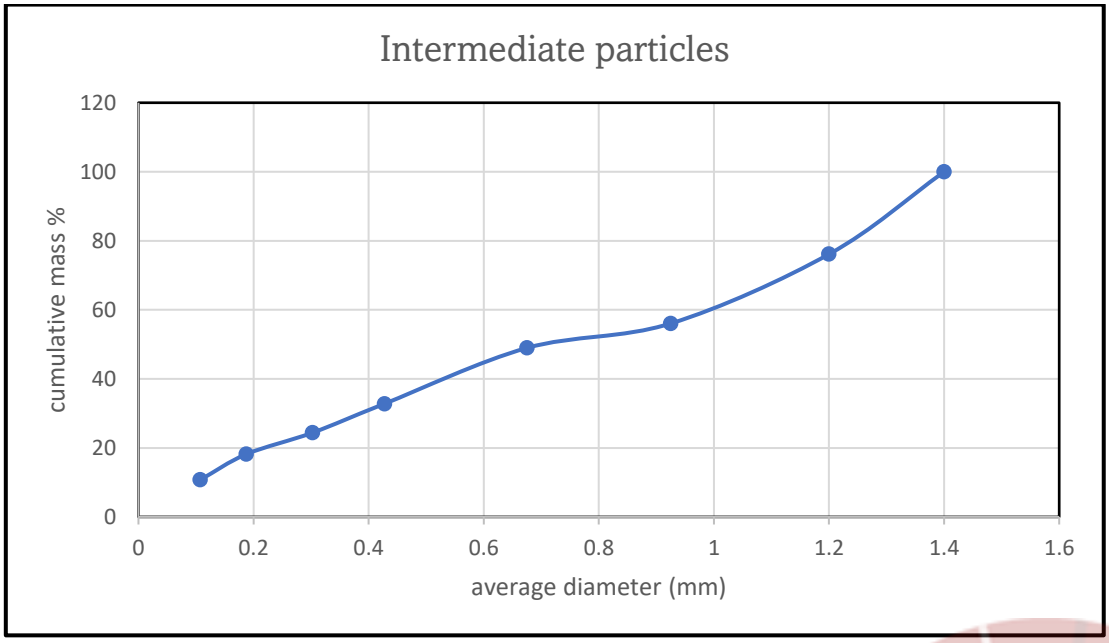

Figure 2 :Accumulative mass percent for intermediate particles

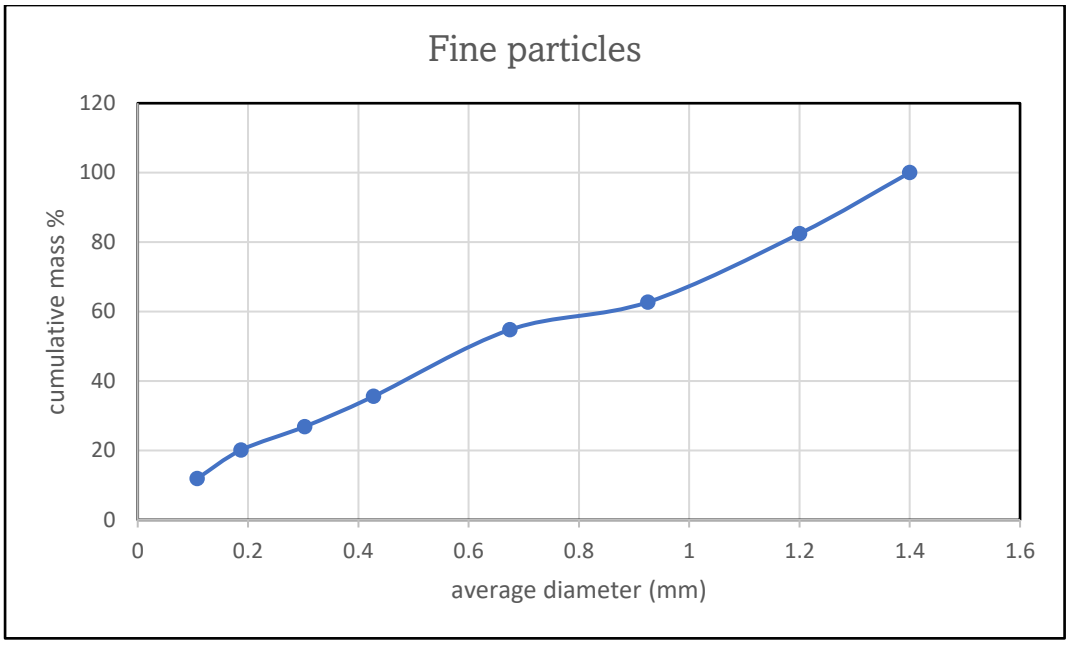

Figure 3:Accumulative mass percent for fine particles

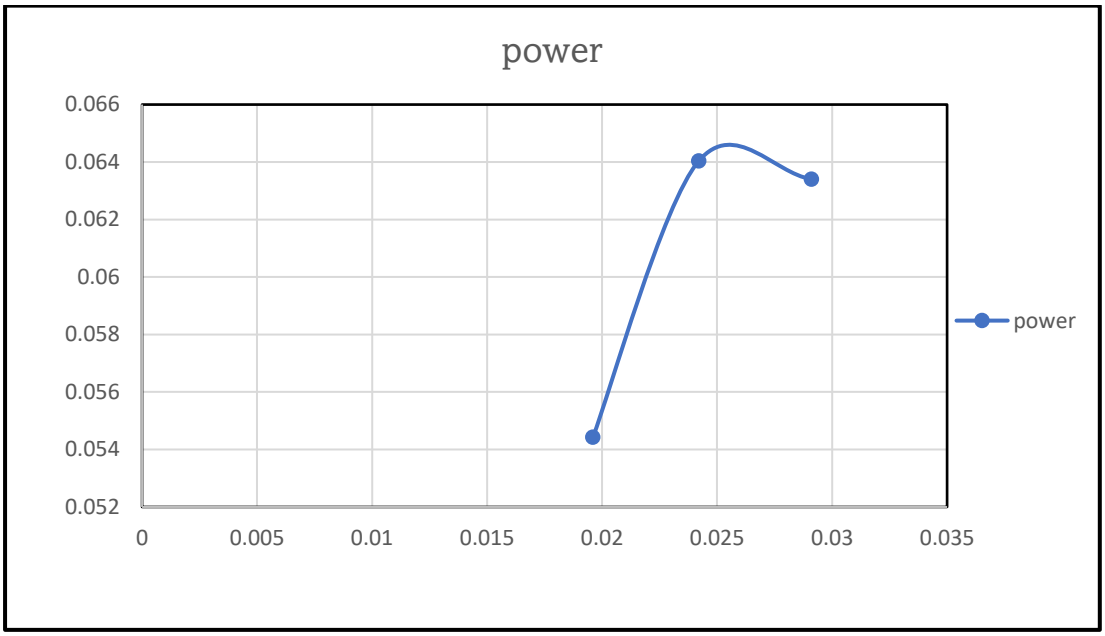

Figure 4:Power required for crushing Vs size for feed particles

Discussion

There are many factors affected the crushing process, including the size of the particles and the time spent in the crushing process. The results showed that the time taken in the crushing was directly proportional to the size of the particles, coarse particles took longer because the size of the particles is larger and thus more cohesive.

The results showed that the relationship between power absorbed by the sample to crush was directly proportional to the size of the particles, so the power of the coarse particles is the largest, and this is related to the crushing time as well.

Figures 1, 2 and 3 showed that the relationship between the cumulative weight and the size of the particles is a direct relationship because when the size is larger, therefore a larger diameter and greater weight.

Figure 4 shows that with increased feed particle size, the power increased to a maximum value and then decreased.

There was a source of error in the experiment, which is that the time spent on crushing the coarse particles was not enough, and this affected the value of the final weight of the sieves it was not equal to the weight that was weighed before crushing and the power less than intermediate.

Conclusion

After conducting this experiment, it was found that there's a direct relationship between the required crushing power and the crushing strength of the oil shale, as well as the size of particles.

- As the particles are coarse, more crushing power is needed to complete grinding.
- The crushing process is affected by several factors, including Size of the raw material, setting of the jaw gap, and crushing technique.
- Oil shale stone sizes are the only variable in this experiment; all other factors, including initial material size, jaw gap setting, and material type, are held constant.

References

1)Chemical engineering laboratory “2” (0915461); University of Jordan; faculty of engineering and Technology; Department of Chemical engineering.

2) Lowrison, C.C., "Crushing and Grinding" Butterworths (1974).

3) McCabe, W.L. and Smith, J.C,"Unit Operation of Chemical Engincering ", 3rd edition, McGraw-Hill

4) Coulson J.M and Richardson J. F., "Chemical Engineering", Volume 2,2nd edition, Pergamon pre

Appendix

sample of calculation, taking the first row from Table (1): Coarse size

- Average volume particles size:

$$V_{avg} = \frac{(4.8+3+2.5+1.68)}{4} = 2.995\ cm^3$$

- Equivalent volume diameter:

Assume particle shape are sphere.

$$d_v = \frac{1}{6}\pi * d^3 \quad \Longrightarrow d = \sqrt[3]{\frac{6*V}{\pi}} = \sqrt[3]{\frac{6*2.995*1000}{\pi}} = 17.88\ mm$$

- Weight of sample (ton):

m=350.8 g

$$\frac{350.8}{1000} * 0.001\ ton = 0.0003508\ ton$$

- Time (hr):

t = 43.22 sec

$$\frac{43.22}{(60*60)} = 0.01201\ hr$$

- Feed rate (ton/hr):

$$\dot{m} = \frac{weight\ of\ sample\ (ton)}{Time(hr)} = \frac{0.0003508}{0.01201} = 0.02914238\ ton/hr$$

- Bonds' work index (kw.hr/ton): 15.8

Applying bonds' law:

$$\frac{p}{\dot{m}} = 0.3162 w_i \left(\frac{1}{\sqrt{L2}} - \frac{1}{\sqrt{L1}}\right)$$

$$\frac{p}{0.02914238} = 0.3162 * 15.8\left(\frac{1}{\sqrt{17.88}} - \frac{1}{\sqrt{1.3}}\right) = 0.063404177 Kw$$

- **From Table (2), taking the fourth row:**

  Average screen opening:

  $d = \frac{(850+500)}{2} = 675\ \mu m/1000 = 0.657 mm$

- Actual sample weight:

wt = 82.5+57.6+17.5+47+23.3+17.5+21.5+16.1+24.2=307.2 g

- Mass fraction %:

  $X = \frac{17.5}{307.2} * 100 = 5.6\%$

- Accumulative weight percent of product:

= 7.8+5.2+6.9+5.6+7.5+15.2=48.6%

Raw data

Jaw Crusher Data Sheet

	Coarse size	Intermediate size	Fine size
Dimensions of feed particle	3 × 2 × 0.8	2 × 1.5 × 0.4	1 × 0.7 × 0.1
	1.5 × 2 × 1	2.7 × 1.5 × 0.4	0.6 × 0.3 × 0.7
	2.5 × 2 × 0.5	1.8 × 1.1 × 0.5	1.2 × 0.5 × 0.4
	3 × 1.4 × 0.4	2.5 × 1 × 0.1	0.9 × 0.3 × 0.1
Weight of sample	350.8	350.5	350
Time need for crushing	43.22 (s)	52.19 (s)	1.07 (min)

	Mass collected on sieve (g)		
Sieves size	Coarse size	Intermediate size	Fine size
X > 1.4	82.5	81.7	60.0
1.4 > X > 1	57.6	68.7	67.2
1 > X > 850	17.5	24.3	27.1
850 > X > 500	47.0	55.3	65.5
500 > X > 355	23.3	28.7	29.7
355 > X > 250	17.5	21.3	23.0
250 > X > 125	21.5	25.4	28.1
125 > X > 90	16.1	10.2	10.8
X < 90	24.2	26.6	29.7
total	307.05	342.2	341.1

Instructor sign: Rula Mustafa

Date: 28/3/2023

Page 33 of 48

The University of Jordan

School of Engineering

Chemical Engineering Department

Chemical Engineering Laboratory (2) (0915461)

Experiment Number 7

Gravity sedimentation

Type of the report: short report

Done by:

Instructor:

Eng. Rula Mohammad

Performing Date: 4/ 04 / 2023

Submitting Date: 11 / 04 / 2023

Abstract

In conventional water treatment systems, flocculation comes first and is followed by sedimentation or gravity separation. Its goal is to improve filtering by getting rid of particulates. A basin must have water flowing through it at a slow enough rate to allow sediment to settle to the bottom of the basin before the water is allowed to flow out of it. A rectangular, square, or circular settling basin is among the equipment needed for this procedure. A sludge collection system, as well as input and outlet structures, are included in the basin's design. Additionally, tube or plate settlers are an optional component of sedimentation systems that might enhance performance.

Table of Contents

Table of Figures

Table of Tables

Results

Table 1: Results of calculation.

Co	100.0	150.0	200.0
Zo	21.4	20.0	18.8
Zc	5.5	10.5	16
tc(min)	25.0	35.0	21.8
tc(s)	1500.0	2100.0	2520.0
Vc(cm/min)	0.3160	0.2171	0.1000
Zi	13.40	18.10	18.70
CL	159.70	165.75	201.07
Z min	8.0	1.9	0.1

Table 2: calculations for the minimum area of thikner

uc= slope (cm/min)	2.20E-01
uc= slope (m/s)	0.000037
Qo (l/day)	3.79E+06
Qo (m3/s)	0.0175
Cu (g/l)	700
A(m2)	230.67

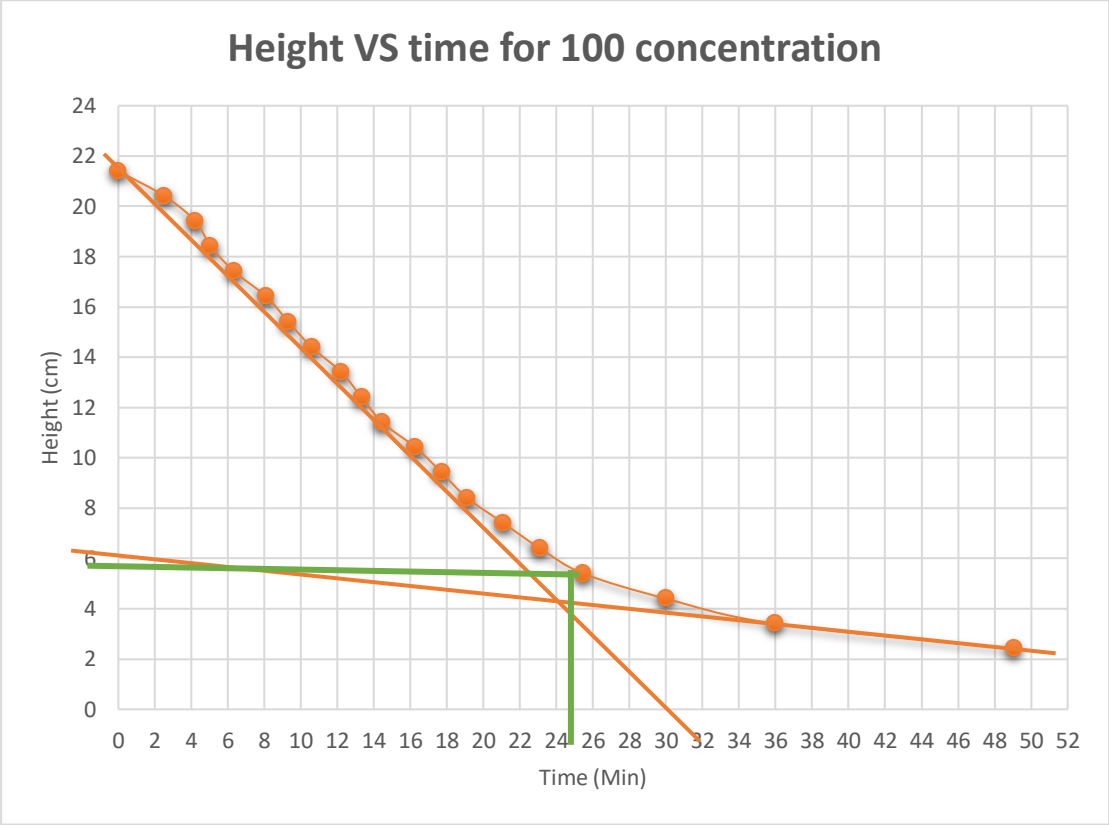

Figure 1: Interface profile of 100g/L concentration sample

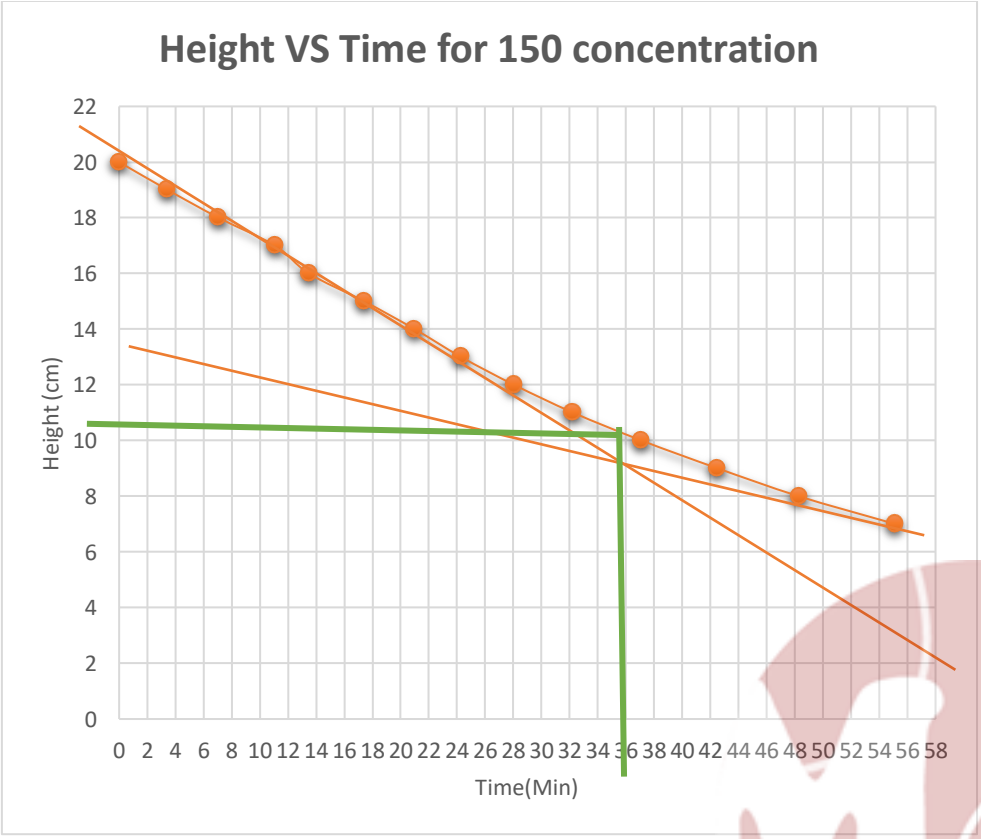

Figure 2:Interface profile of 150g/L concentration sample

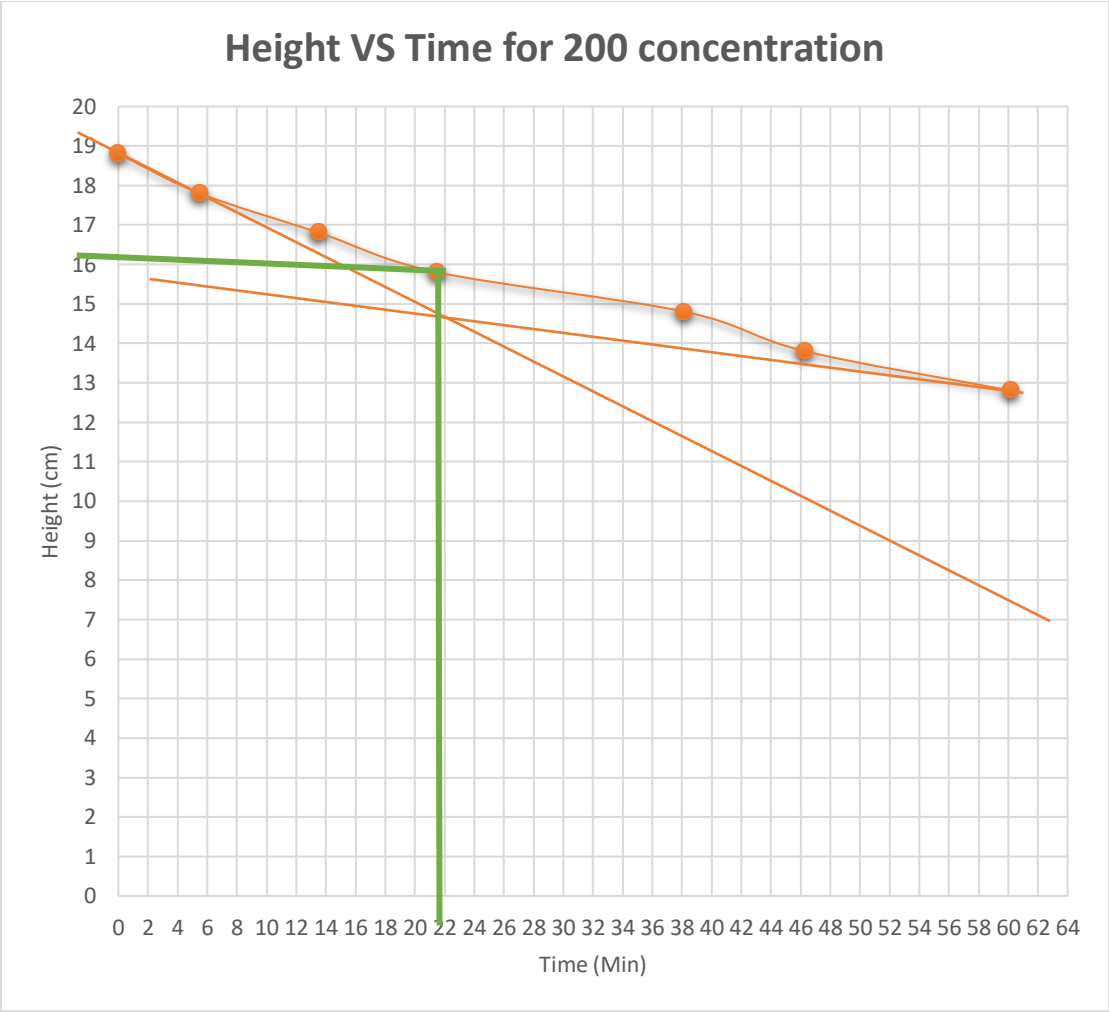

Figure 3:Interface profile of 200g/L concentration sample

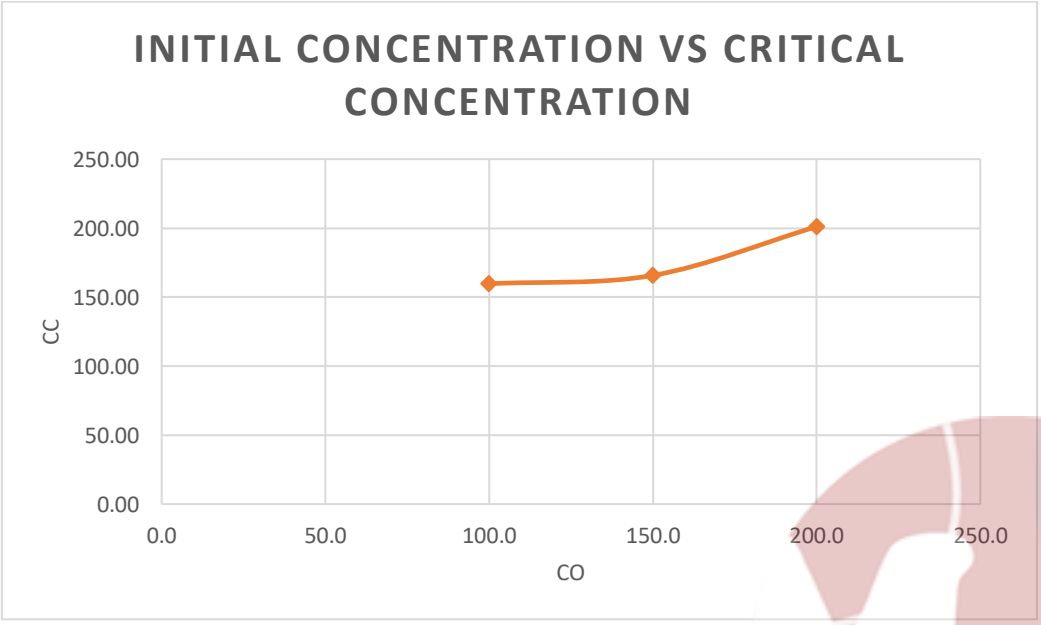

Figure 4:Initial concentration vs critical concentration

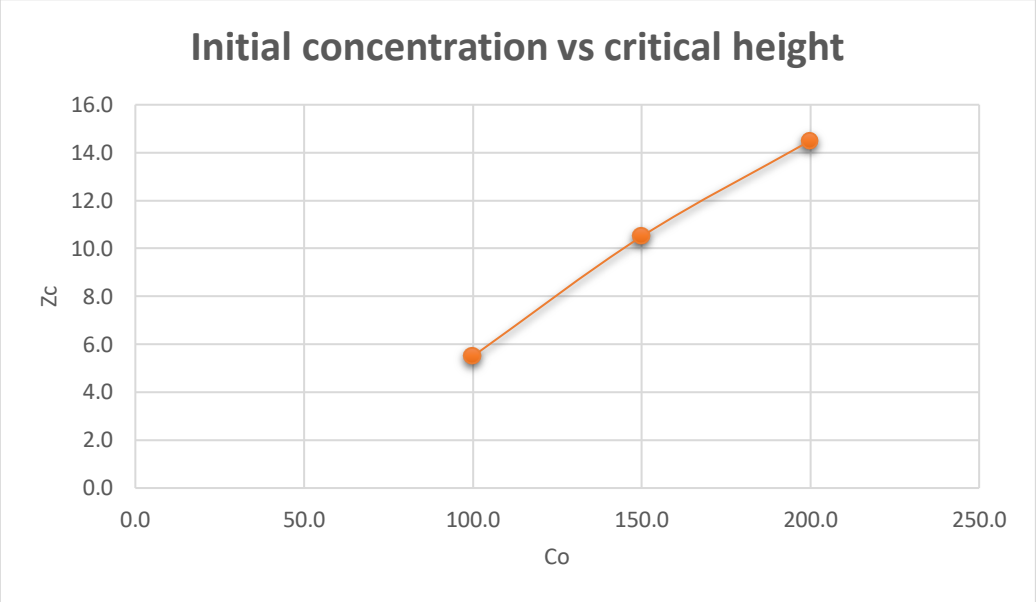

Figure 5:Initial concentration vs critical height

Discussion

In this experiment, we studied how sand settles in water. Three graded cylinders that are identical but have varied solid concentrations make up the apparatus.

The results shows that the sedimentation rate which is the rate of change of height of the interface between the clear liquid and the settling slurry interface is directly proportional to the difference between the interfacial heights until the critical height is reached at the critical time. As shown in table (1) and figures (1 & 2 & 3) the rate of sedimentation of the sand increases when the concentration of the suspension decreases, which means increasing the mass of the suspended solid was required time greater than that lighter sample.

Also, as shown in figures (4 & 5) the relation between Initial concentration vs. critical height and Initial concentration vs. critical concentration, respectively, both relations were directly proportional.

Conclusion

The sedimentation process is affected by many factors such as, diameter of cylinder, height, concentration and particle size.

Increasing the concentration of suspended solids take more time to settle, Sedimentation rate is directly proportional to the difference between the interfacial heights, The rate of sedimentation of the sand increases when the concentration of the suspension decreases, The Initial concentration is directly proportional to the critical height, The Initial concentration is directly proportional to the critical concentration.

References

1)*Chemical engineering laboratory "2" (0915461); University of Jordan; faculty of engineering and Technology; Department of Chemical engineering.*

3) *McCabe, W.L. and Smith, J.C,"Unit Operation of Chemical Engincering ", 3rd edition, McGraw-Hill*

4) *Coulson J.M and Richardson J. F., "Chemical Engineering", Volume 2,2nd edition, Pergamon pre*

Appendix

For Sample 1:

Given initial concentration and initial height:

$C_0 = \frac{100g}{L}$, $Z_0 = 21.4$ cm

From the intersection of the tangent lines on the height VS time graph for sample 1, critical height and critical time is obtained:

$Z_C = 5.5\text{cm}, t_C = 25$ min

Finding settling velocity:

$V_C = \frac{Z_C}{t_C} = \frac{5.5}{25} = 0.3160 \frac{\text{cm}}{\text{min}}$.

$Z_i = Z_C + U_C t_C = 5.5 + 0.3160 * 25 = 13.4$ cm.

Critical concentration:

$C_C = \frac{C_o Z_O}{Z_i} = \frac{100*21.4}{13.4} = 159.7$ g/L

Minimum height:

$Z_{min} = Z_o - Z_i = 21.4 - 13.4 = 8$ cm

Minimum thickener area:

$$A = \frac{Q_o C_o}{U_c} * \left(\frac{1}{C_C} - \frac{1}{C_U}\right) = 0.0175 * 100 * \frac{1}{.000037} * \left(\frac{1}{159.70} - \frac{1}{700}\right) = 230.67 \text{ m}^2$$

❖ Data Sheet

Version no. 7 September, 2020

Gravity Sedimentation Data Sheet

→ 21.4 100 20 150 18.8 200

	Conc.= 100	Conc.= 150	Conc.= 200
Height	Time	Time	Time
	2:54	3:45	1cm = 5:48:11
	4:22	7:07	1cm = 13:54:60
	5:07	11:08	1cm = 21:51:30
	6:36	13:48	1cm = 21:25:30
	8:12	17:41	1cm = 38:18:
	9:32	21:00	1cm = 46:30
	10:59	24:30	1cm = 1:2
	12:22	28:06	1:10
	13:33	32:26	
	14:47	37:12	
	16:30	42:53	
	17:37	48:29	
	19:12	55:15	
	21:10	1:02:21	
	23:10	1:09:34	
	25:47	1:18:07.	
	30:00		
	36:14		
	49:07		
	1:19:07	4/4/2023	

Page 37 of 48

The University of Jordan

School of Engineering

Chemical Engineering Department

Chemical Engineering Laboratory (2) (0915461)

Experiment Number (8)

Ball mill

Type of the report: short report

Done by:

Instructor:

Eng. Rula Mohammad

Performing Date: 16/ 05 / 2023

Submitting Date: 22 / 05 / 2023

Abstract

In this experiment, a cylindrical steel drum was used with a stack of steel balls in it. The drum was rotated at a fixed speed, and a sample of coarse oil shale was added to it. The aim of the experiment was to observe the effect of ball milling on the particle size. The experiment was conducted for a set duration of time, after which the sample was collected and analyzed using different techniques such as sieving. The results showed that ball milling reduced the particle size of the oil shale.

Table of Contents

Table of Figure

Table of Tables

Result

Table 1 : Result for sample 1

Diameter (µm)	average diameter (µm)	weight of sample#1	mass fraction%	cumulative weight %
			0	100
x > 500	500	33.4	34.25641026	65.74358974
355< x <500	427.5	12.8	13.12820513	52.61538462
250 < x < 355	302.5	7.6	7.794871795	44.82051282
125 < x < 250	187.5	8.9	9.128205128	35.69230769
90< x < 125	107.5	2.3	2.358974359	33.33333333
63<x < 90	76.5	32.5	33.33333333	0
Total		97.5	100	232.2051282

Table 2 : Result for sample 2

Diameter (µm)	average diameter (µm)	weight of sample#2	mass fraction%	cumulative weight %
			0	100
x > 500	500	69.5	70.55837563	29.44162437
355< x <500	427.5	3.4	3.45177665	25.98984772
250 < x < 355	302.5	2.9	2.944162437	23.04568528
125 < x < 250	187.5	14.9	15.12690355	7.918781726
90< x < 125	107.5	3.4	3.45177665	4.467005076
63<x < 90	76.5	4.4	4.467005076	2.66454E-14
Total		98.5	100	90.86294416

Table 3 : Result of bond's law

	sample#1	sample#2
Feed particle size (µm)	500	850
avg feed particle (mm)	0.5	0.85
weight (g)	100	100
weight (ton)	0.0001	0.0001
time (min)	16	16
time (hour)	0.266666667	0.266666667
Rotation speed (rpm)	355	355
power consumption (W)	18	22
power consumption (KW)	0.018	0.022
feed rate (ton/hr)	0.000375	0.000375
Bond's work index (KW.hr/ton)	13.46552164	141.4129697

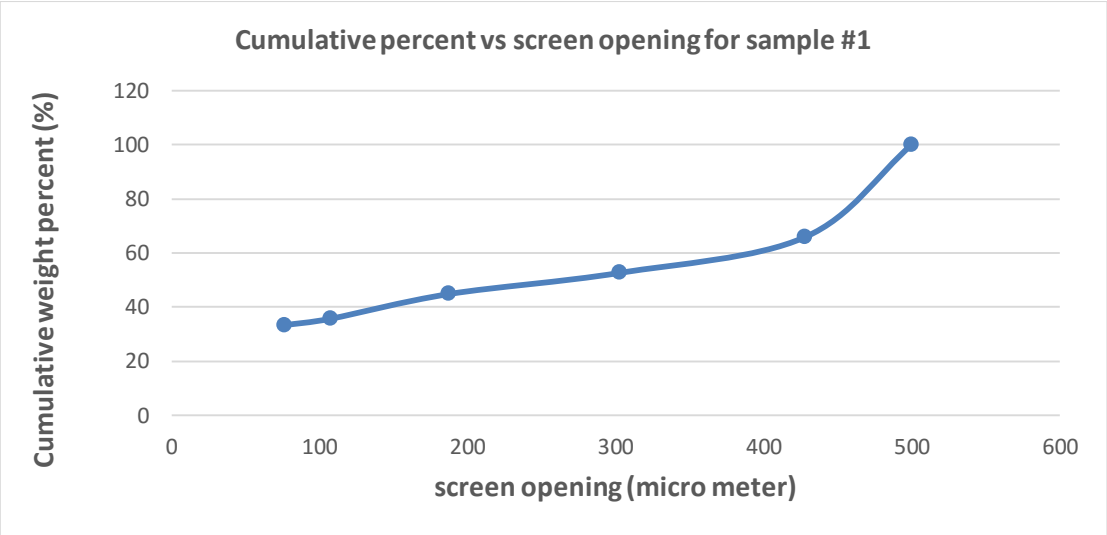

Figure 1 : Cumulative percent vs screen opening for sample 1

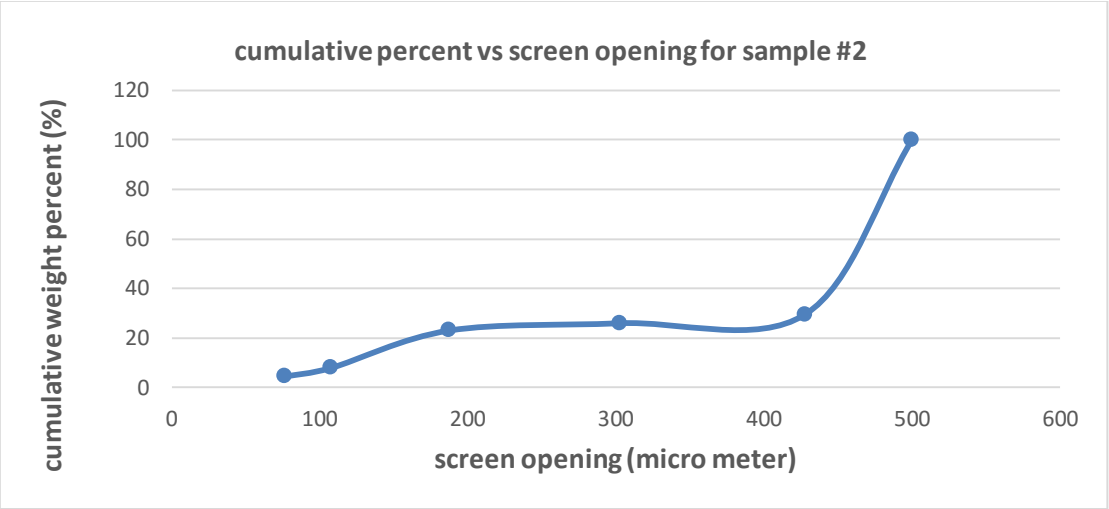

Figure 2 : Cumulative percent vs screen opening for sample 2

Discussion

During the oil shale particle milling process, scarching All other factors are constant, with the exception of milling duration, which has a variable effect on particle size. Start putting oil shale with an average diameter of 850 and 500 micrometers inside the cylinder, where the number of balls inside and the rotation's speed are two variables that never change in order to increase the milling process because the driving power will be greater. Various-sized balls are inside. The first sample takes five minutes, the second takes ten, and the final sample takes fifteen. To determine the size of the particles still present after the grinding process, the product is placed through sieves once the miiling process is complete.During the oil shale particle milling process, scarching All other factors are constant, with the exception of milling duration, which has a variable effect on particle size. In order to enhance the milling process mass, the number of balls inside the cylinder and the rate of rotation are two variables that never change.

Figure 1, shows that size reduction increases as milling duration increases because of the various grinding settings, as can be seen from the data, there is a percentage error between the experimental and theoretical bond work index.During the oil shale particle milling process, scarching All other factors are constant, with the exception of milling duration, which has a variable effect on particle size.

Conclusion

In this experiment we conclude that:

- There are some variables that affect milling process such as: ball size and volume share, speed of cylinder, type of materiel, time and the Properties of material to be ground (hardness, viscosity).

- Size reduction rises as ball milling power increases.

- A lower weight was required after ball milling since: some particles were lost during the process of removing them, when screen opening increases, the cumulative weight percentage of the product is determined.

- accumulative mass passing increases as screen opening increases.

- Power consumption decreases with increases of feed particle size at constant time.

References

1)Chemical engineering laboratory “2” (0915461); University of Jordan; faculty of engineering and Technology; Department of Chemical engineering.

2) McCabe, W.L. and Smith, J.C,"Unit Operation of Chemical Engincering ", 3rd edition, McGraw-Hill

3) Coulson J.M and Richardson J. F., "Chemical Engineering", Volume 2,2nd edition, Pergamon pre

Appendix

For sample 1, raw 2

-Feed particle size= 500µm.

-Weight of sample= 100 g

-Time= 16min

-Speed= 355 rpm.

-Power= 22W

-Mass fraction= $\frac{3.4}{100} = 0.034$

-Cumulative weight= $m_1 + m_2 = 69.5 + 3.4 = 72.9g$

-Cumulative wt. fraction= $\frac{\text{cumulative weight}}{\text{Total cumulative weight}} = \frac{72.9}{100} = 0.729$

-Feed in tons= $100 * 10^{-5} tons$

-time= 16/60= 0.26hr

-Feed rate= $\frac{100*10^{-5}}{0.26}$= 0.00038 ton/hr

-Power= 0.022 kW

-from Bonds law: Work index: (experimental) (from row 1)

$$W = \frac{\left({}^{P}/_{m}\right)*\left({}^{1}/_{0.3162}\right)}{\left(\frac{1}{\sqrt{L_2}} - \frac{1}{\sqrt{L_1}}\right)} = \frac{\left({}^{0.018}/_{0.000375}\right)*\left({}^{1}/_{0.3162}\right)}{\left(\frac{1}{\sqrt{97.5*10^{-5}}} - \frac{1}{\sqrt{232.2*10^{-5}}}\right)} = 13.4 \text{ kW.h/ton.}$$

Ball Mill Data Sheet

	Sample #1	Sample #2	Sample #3
Feed particle size (μm)			
Weight of sample (g)	100g	100g	
Time (min)	16	16	
Rotation speed (rpm)	355	355	
Power consumption (W)	22	18	

	Mass collected on sieve (g)					
Sieves size	Sample #1	Mass fraction %	Sample #2	Mass fraction %	Sample #3	Mass fraction %
> 500	69.5		33.4			
500 > x > 350	3.4		12.8			
350 > x > 250	2.9		7.6			
250 > x > 125	14.9		8.9			
125 > x > 90	3.4		2.3			
Pan	4.4		32.5			
Total	98.5		97.5			

Instructor sign:	
Date:	16/5/2023